

2008

Improved Consistency of Resistance Spot Welding via Power Supply Control Strategy

Jing Bai

Follow this and additional works at: <https://ir.lib.uwo.ca/digitizedtheses>

Recommended Citation

Bai, Jing, "Improved Consistency of Resistance Spot Welding via Power Supply Control Strategy" (2008). *Digitized Theses*. 4819.
<https://ir.lib.uwo.ca/digitizedtheses/4819>

This Thesis is brought to you for free and open access by the Digitized Special Collections at Scholarship@Western. It has been accepted for inclusion in Digitized Theses by an authorized administrator of Scholarship@Western. For more information, please contact wlsadmin@uwo.ca.

Improved Consistency of Resistance Spot Welding via Power Supply Control Strategy

(Spine title: Improved Consistency of RSW via Power Supply Control
Strategy)

(Thesis format: Monograph)

by

Jing Bai

Graduate Program
in
Engineering Science
Electrical and Computer Engineering

A thesis submitted in partial fulfillment
of the requirements for the degree of
Master of Engineering Science

School of Graduate and Postdoctoral Studies
The University of Western Ontario
London, Ontario, Canada

© Jing Bai 2008

Certificate of Examination

THE UNIVERSITY OF WESTERN ONTARIO
SCHOOL OF GRADUATE AND POSTDOCTORAL STUDIES
CERTIFICATE OF EXAMINATION

Chief Adviser:

Dr. Lyndon Brown

Examining Board:

Dr. Jin Jiang

Advisory Committee:

Dr. Robert Sobot

Dr. Shaun Salisbury

The thesis by

Jing Bai

entitled:

**Improved Consistency of Resistance Spot Welding via Power Supply
Control Strategy**

is accepted in partial fulfillment of the
requirements for the degree of
Master of Engineering Science

Date: _____

Chair of Examining Board
Dr. Serguei Primak

Abstract

Resistance spot welding (RSW) is widely used as an efficient joining technology for assembling metal components in the automotive, biomedical and electronics industry. The demand for improved welding consistency has led to switching from voltage control to current control. In addition, commercially available micro-spot welders may also provide power control mode.

Power can be interpreted as the square root of the geometric mean of voltage and current. From this view point, the three existing power strategies can be seen as differently weighted geometric means of voltage and current. In fact, any weighted mean of voltage and current can be used as a viable control variable. Based on this insight, it is recognized that there should be one specific weighted mean of voltage and current that can lead to the least variance in the weld process. This provides a new tool for the weld engineer to maximize the quality of their welding processes. For welding 0.152mm gauge stainless steel, a 40% weighting on the voltage produced the most consistent weld nugget diameter was found. And with this control parameter, a 60% improvement in variance in weld nugget size versus constant current control was achieved.

keywords: weighted-mean of voltage and current, control variable, resistance spot welding.

Acknowledgement

I would like to express my sincere gratitude to my supervisor, Dr. Lyndon J. Brown of The University of Western Ontario for his guidance and support on this research and thesis work, for his concern on all aspect of my study at The University of Western Ontario.

I would like to thank Dr. Norman Zhou, Dr. Michael Kuntz of the University of Waterloo for their technical guidance and unlimited use of their facilities. I also like to appreciate my colleagues in our research group for the discussion and support.

My special appreciation goes to my family and friends for their encouragement and optimistic outlook.

Table of Contents

Certificate of Examination	ii
Abstract	iii
Acknowledgement	iv
List of tables	vii
List of figures	viii
1 Introduction	1
1.1 Introduction	1
1.2 Research Motivation and Objective	2
1.2.1 Problems and Proposed Solution	2
1.2.2 Contribution of This Thesis Work	4
1.3 Outline of This Thesis	5
2 Background Knowledge on Resistance Spot Welding	6
2.1 Welding Sequence and Classification	6
2.2 Resistance Spot Welding Process Review	8
2.2.1 Heat Generation and Dynamic Resistance	9
2.2.2 Review of Existing RSW Power Supplies	15
2.2.3 Resistance Spot Welding Sequence	18
2.2.4 Signals Commonly Monitored during Welding Process	23
2.3 Small Scale RSW and Micro-RSW	25
3 Control Strategy Design for Resistance Spot Welding	29
3.1 Definition of the Geometric Mean	29
3.2 Control Strategy Design	30
3.3 Open Loop Voltage Control Mode	32
3.4 Comparison for Different Control Schemes	33

4	Spot Welding System Description	36
4.1	Technical Requirement	36
4.2	System Description	37
4.2.1	Power Section	38
4.2.2	Control Electronics	38
4.2.3	Dspace Control System	39
5	Application of Strategy to Welding 0.152mm Gauge Stainless Steel	41
5.1	Experimental Setup	42
5.2	Lobe Test for Open Loop Voltage Control Mode	45
5.2.1	Weld Lobe	45
5.2.2	Tensile Test	46
5.2.3	Peel Test	46
5.2.4	Lobe Test for Open Loop Voltage Control Mode	48
5.3	Step Test for Constant Current Control Mode	50
5.4	Determining Set Point for each α	55
5.5	Variance Calculations	56
6	Experimental Analysis and Results	58
6.1	Lobe Test for Open Loop Voltage Control Mode	58
6.2	Step Test for Constant Current Control Mode	59
6.3	Determining Set Point for each α	63
6.4	Experimental Data Analysis	64
6.5	Summary of The Experiments	68
7	Conclusion and Future Work	70
7.1	Summary of Achievements	70
7.2	Future Work	71
	Bibliography	73
	Appendices	
A	Experimental Results for Different Control Schemes	76
	Curriculum Vita	81

List of Tables

2.1	Classification of welding processes	27
2.2	Comparison between LSRSW, SSRSW and Micro-RSW	28
3.1	The generic control and other control modes	32
4.1	Technical requirements	36
5.1	Mean nugget size at different current set points	56
5.2	Set points at different α value	56
6.1	PI controller gains value at corresponding set points	64
6.2	Mean nugget diameter at different set points	65
6.3	Control variables under the control modes	67

List of Figures

2.1	The occurrence of resistances in electrical RSW	9
2.2	Lumped parameter model of the secondary circuit for RSW	11
2.3	Schematic showing the change in resistance during RSW	12
2.4	Theoretical dynamic resistance curve	14
2.5	Schematic of current waveforms of CD, DC and AC power supplies	15
2.6	The procedure of RSW	19
2.7	Schematic of a typical RSW monitoring and control system	23
3.1	Generic power control mode	31
3.2	Block diagram of open loop voltage control mode	33
3.3	Experimental results for the open loop voltage control mode	34
3.4	Experimental results for the pure current control mode	34
3.5	Experimental results for the constant power control mode	35
4.1	Resistance spot welding system	38
4.2	Sensing circuit for output current	39
4.3	Mechanic structure of the current sensing circuit	40
5.1	Typical resistance under voltage control and current control	42
5.2	Block diagram of experimental set-up	43
5.3	(a) Tensile test sample (b) peel test sample	44
5.4	Tensile test for measuring weld strength	46
5.5	Peel test for measuring nugget diameter	47
5.6	Schematic showing joint failure modes during peel test	48
5.7	A weld lobe diagram	49
5.8	Step test input and output	51
5.9	Plot of current and duty cycle step test	54
5.10	Block diagram for the PI controller tuning	54
6.1	(a) Weld strength and (b) nugget diameter versus welding time	60
6.2	Effect of expulsion on dynamic resistance curve	61
6.3	Lobe curve for open loop voltage control mode	62
6.4	PI controller tuning for current control mode	62
6.5	Mean nugget diameter for different current setting	63
6.6	Variance comparison in (a) weld strength and (b) nugget diameter	66
6.7	Variance comparison in control variables at each of α	67
A.1	Experimental results for the control mode with $\alpha = 0.1$	77

A.2	Experimental results for the control mode with $\alpha = 0.2$	77
A.3	Experimental results for the control mode with $\alpha = 0.3$	78
A.4	Experimental results for the control mode with $\alpha = 0.4$	78
A.5	Experimental results for the control mode with $\alpha = 0.6$	79
A.6	Experimental results for the control mode with $\alpha = 0.7$	79
A.7	Experimental results for the control mode with $\alpha = 0.8$	80
A.8	Experimental results for the control mode with $\alpha = 0.9$	80

Chapter 1

Introduction

1.1 Introduction

Resistance spot welding (RSW) is the key metal joining technique for high volume production in the automotive, biomedical and electronics industry. RSW is a process in which faying surfaces are joined in one or more spots by the heat generated by resistance to the flow of electric current through workpieces that are held together under force by electrodes. The contacting surfaces in the region of current concentration are heated by a short time pulse of high-amperage current to form a fused nugget of weld metal. When the flow of current ceases, the electrode force is maintained while the weld metal rapidly cools and solidifies. The electrodes are retracted after each weld, which usually is completed in a fraction of a second. With an average of two to five thousands spot welds performed on each manufactured car leading to 100 billion spot welds per year in the North America automobile industry, RSW has become the predominant means of auto body assembly [1]. And for increasing application of very thin metal sheets in manufacturing electronic components and devices, small-scale resistance spot welding (SSRSW) is attracting more and more researchers attention [2].

In fact, weld quality is the center of all aspects of welding. Hence, a material, before it is used in production, needs to be qualified as weldable; namely, that using

standard welding equipment and schedules would yield welds of sufficient size and strength quality. RSW differs from other forms of welding in that no extra material is used, such as filler rod in arc welding; hence it is not complicated by the addition of extra material. However, the melting process is entirely contained within the workpieces, thus observation and measurement are severely constrained. And there are no universally accepted standards of weld quality. Therefore, for the sole purpose of assuring the quality of the spot weld, the primary objective of the spot welding research has been to monitor and control the process [3, 4].

1.2 Research Motivation and Objective

1.2.1 Problems and Proposed Solution

In previous research, the electrical current or voltage [5], weld force [6] and dynamic resistance [7] signals have been indicated as being the most used in monitoring and control systems to evaluate weld quality. Based on either information obtained from the monitoring and/or modeling, control algorithms have been developed to control the process for assuring quality welds. However, market penetration of these algorithms has been poor, often because the algorithms are not robust for real conditions on a shop floor. The approach presented here has advantages of simplicity and requires little modification of existing practice.

Many papers have been published for resistance spot welding weld quality with different control schemes [8, 9], including open loop control, constant current control and constant power control.

Traditional control of the welding operation is open-loop and weld engineers preselect appropriate values for timing parameters, including firing angles of silicon

controlled rectifiers. Initial improvement included adjusting the timing parameters to account for line voltage variations [10].

The resistances across the workpieces are extremely low, often in the 10s of uohms for large scale spot welding and in the few milliohm for small scale spot welding. This is of the same order as both the source resistance of power supply and weld cables. Further any movement of the weld cable can have significant impact on its impedance. Thus control of the voltage at the power supply does not provide good control of the power delivered to the weld. And spatter is increased when the generated heat is arbitrarily varied. Many of these sources of variability are reduced by using active feedback to regulate the current supplied by the weld power supply. Thus the demand for highly improved welding consistency has led to switching from open loop control to current control by using electrical feedback to regulate a constant current that can reduce heating variance during the formation of a weld [11].

Nevertheless, in the constant current control method for resistance spot welding system, the generated heat is varied due to the change of the specimen resistance. Similar to the output voltage, the welding current itself does not represent the input heat either. In order to determine the heat input to a weld, both voltage and current must be measured. Therefore, controllers based on the so-called constant power control algorithm have been developed and are now commercially available. As the result, the generated heat can be kept constant, resulting in less spatter [12]. However, the constant power controls are still not perfect. Generally the voltage is measured at the power supply instead of at the weld. In practice, as discussed later it is not practically possible at this point in time to measure voltage at the weld with most large scale welders. Further, because some of the current passes through adjacent welds and outside of the electrodes, the measured current is larger than the effective current. Thus some other measure of power should be able to lead to more consistent

welds.

In mathematics, the geometric mean is defined as a type of mean or average, which indicates the central tendency or typical value of a set of numbers. The geometric mean of n numbers is formed by the n^{th} root of their product. Thus the geometric mean of voltage and current is $(VI)^{\frac{1}{2}}$, i.e. the square root of the power. A weighted geometric mean of variables V and I would be given by $V^{1-\alpha}I^\alpha$ where $0 \leq \alpha \leq 1$ is the weighting. It is proposed that any weighted geometric mean of voltage and current is a viable control variable and that this approach unifies the existing constant current ($\alpha = 1$), constant power $\alpha = \frac{1}{2}$ and constant voltage $\alpha = 0$ strategies.

Therefore, the objective of this thesis is to investigate the selection of the control variable proposed in a generic power control mode to achieve the most consistent welds experimentally and through optimization of uncertainty models. To demonstrate this strategy, it will be applied to the welding of 0.152mm thick stainless steel.

1.2.2 Contribution of This Thesis Work

The aim for this thesis is to present a new power supply strategy to improve the consistency of resistance spot welding for every spot weld. Since controlling heating at the nugget is the key element for assuring weld quality, and heating is a product of voltage at the weld and current through weld, neither of which is measurable, the right combination of measurable current and measurable voltage to control will be investigated. To the best of our knowledge, no previous study of this type has been published.

In this thesis, any weighted mean of voltage and current can be used as a viable control variable. And changing control variable affects the consistency of welding

process. Hence there should be one specific weighted mean of voltage and current that can lead to the least variance in the weld process. This provides a new tool for the weld engineer to maximize the quality of their welding processes. For one case study we found that 40% weighting on the voltage produces the most consistent welds. And as shown in the experimental result figures in chapter 6, approximately 60% improvement in variance in weld nugget size versus constant current control was achieved.

1.3 Outline of This Thesis

The thesis is organized as follows:

Chapter 1 gives a brief introduction of the resistance spot welding (RSW) and presents the contribution and the structure of this thesis. In chapter 2, a general review of welding process is proposed, the working principle of the RSW and the existing power supplies are described. Chapter 3 presents a novel control strategy for assuring the weld consistency. And in this chapter, different control schemes implemented for the welding process are also studied. After describing the welding system for this study in chapter 4, the application of this new strategy to welding 0.152mm gauge stainless steel is presented in chapter 5. In this chapter, the experimental procedure is provided. Chapter 6 gives the experimental analysis. The welding quality under different control variable has been analyzed based on the experimental results. The test results demonstrate the feasibility of the proposed control strategy. And the stability of the control modes has been analyzed. Chapter 7 concludes the achievements of this thesis and provides suggestions for future work.

Chapter 2

Background Knowledge on Resistance Spot Welding

In order to provide a clear picture on resistance spot welding, some background knowledge is introduced in this chapter. The first section the general principle of welding process is presented to explain the application of welding, and its classification. Next, the resistance spot welding procedure, existing power supplies and typical welding parameter monitoring are described. Finally, the applications of the small-scale and micro-scale resistance spot welding are reviewed.

2.1 Welding Sequence and Classification

Welding is a fabrication process that joins materials, usually metals or thermoplastics, by causing coalescence. This is often done by melting the workpieces and adding a filler material to form a pool of molten material (the weld puddle) that cools to become a strong joint, with pressure sometimes used in conjunction with heat, or by itself, to produce the weld. Many different energy sources can be used for welding, including a gas flame, an electric arc, a laser, an electron beam, friction, and ultrasound.

The American Welding Society definition for a welding process is a materials joining process which produces coalescence of materials by heating them to suitable temperatures with or without the application of pressure or by the application of

pressure alone and with or without the use of filler material. The welding processes has been classified based on the mode of energy transfer and the influence of capillary attraction in effecting distribution of filler metal in the joint as the two main factors. Capillary attraction distinguishes the welding processes grouped under Brazing, Soldering, Arc Welding, Gas Welding, Resistance Welding, Solid State Welding, and Other Processes [13]. Table 2.1 lists the common welding process in their official groupings. This table also shows the letter designation for each process. The letter designation assigned to the process can be used for identification on drawings, tables, etc.

The selection of a specific welding process depends upon many factors, such as the geometric shape, material, size, thickness, costs, portability, and skills needed, etc. The resistance spot welding is widely and commercially used in industries like automobiles, cabinets, aerospace, appliances, etc [13]. In this thesis, the resistance spot welding was studied.

Resistance welding is a joining process belonging to the pressure welding sector. And resistance welding is extensively used for the mass production assembly of the all-steel body and its component sheet metal parts. Its wide adaption has been brought about by its technical advantages and the reduction in cost. There are a number of resistance welding processes as shown in Table 2.1. And resistance spot welding (RSW) is the primary sheet metal welding process in the manufacture of automotive assemblies.

Spot welding is used throughout the industry for two main reasons: first, because it is a strong and reliable method of joining two pieces of metal; and second, because of the total absence of panel distortion through the welding [14]. Besides during the welding process, there is no extra material used, which is different from other welding process, hence it is not complicated by the addition of extra material.

Moreover, since car body design demands careful choice of the sheet metal, tensile strength and ductility which are good in mild steel, are vital to the ability to absorb the impact energy, resistance spot welds are widely used in the automotive sector.

Furthermore, the spot welding is a typical technology of body-in-white fabrication in the automotive industry, and as such it has the benefit of being a well known, extensively proven technology with which the industry is highly familiar and has considerable experience. Other main advantages of spot welding include high operating speeds and suitability for automation or robotization and inclusion in high-production assembly lines together with other fabricating operations. And the attachment of braces, brackets, pads, or clips to formed sheet-metal parts such as cases, covers, bases, or trays is another common application of RSW. With automatic control of current, timing and electrode force, sound spot welds can be produced reasonably and consistently at high production rates and low unit labor costs using semiskilled operators. The resistance spot welding process is especially favored in manufacturing since it involves no direct consumable besides electricity. A resistance spot weld typically requires 15kJ. Since electricity is typically priced in the pennies per $kw \cdot hour$, this involves tiny fractions of a cent as compared to the substantially higher cost of screws or rivets.

2.2 Resistance Spot Welding Process Review

In the spot welding process, two overlapped or stacked stamped components are welded together as a result of the resistance heating caused by the passage of electric current. This is provided by the workpieces as they are held together under pressure between two electrodes as shown in Figure 2.1 [15].

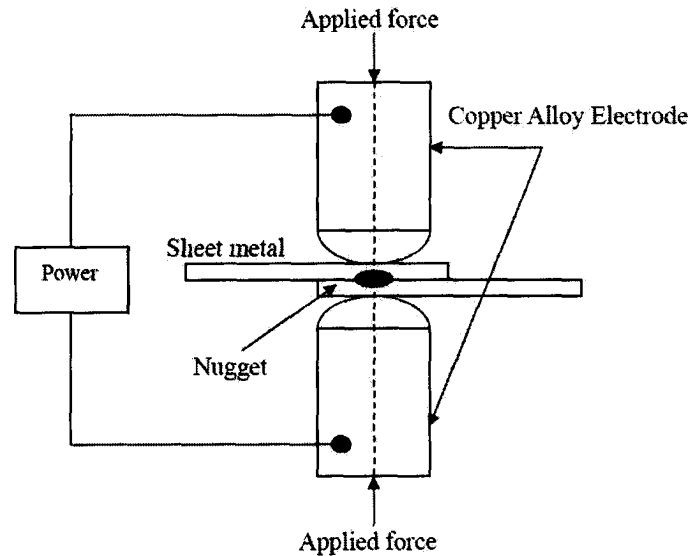


Figure 2.1: The occurrence of resistances in electrical RSW

The copper alloy electrodes are used to apply pressure and convey the electrical current through the workpiece during the formation of nugget. In the spot welding process, a weld nugget will start to form after sufficient energy has been put into the weld zone to raise the material to the solidus-liquidus temperature of the materials to be bonded and hence to begin the formation of a melted weld pool. The size of the nugget formed is determined by the magnitude and duration of the current.

2.2.1 Heat Generation and Dynamic Resistance

The heat needed to create the coherence is generated by applying an electric current through the stack-up of sheets between the electrodes. Therefore, the formation of a welded joint strongly depends on the electrical and thermal properties of the sheet and coating materials. As a weld's formation can be linked to the electrical and thermal processes of welding, controlling the electrical and thermal parameters is a

common practice. The general expression of heat generated in an electric circuit can be expressed as

$$Q = \int I^2 R dt = \int V_t^2 / R dt = \int V_t I dt \quad (2.1)$$

where, Q is the heat generated in the workpieces, I is the welding current, V_t is the voltage at the weld tips and R is the electrical resistance seen at the weld head. This is expressed as an integral over time as it is well known that the resistance, and possibly the current and voltage, vary with time.

In fact, the resistance in the circuit is composed of many sources, which contribute in various degrees to the production of the weld. Figure 2.2 shows a common lumped parameter model of the secondary circuit for resistance spot welding systems. It is seen to consist of a power supply E_s , resistances of the cables R_{sa} and R_{sb} , inductances L_{sa} and L_{sb} , bulk resistances of the upper/lower electrodes R_{1a} and R_{1b} , shunt resistance R_5 that represents the resistance of current flowing around the weld spot and through adjacent welds as well as the load dynamic resistance.

The load resistance is the key component in this circuit, which is a function of the weld force, the materials to be used and temperature during welding. And it consists of the following components as shown in (Figure 2.2):

- bulk resistances of the upper/lower part joints R_{2a} , R_{2b} ,
- contact resistances between the upper/lower electrode and workpiece R_{3a} as well as R_{3b} ,
- contact resistance between the two workpieces R_4 .

The bulk resistance is sensitive to temperature and independent of pressure. For all metals, the bulk resistance increases along with temperature. Therefore, the bulk

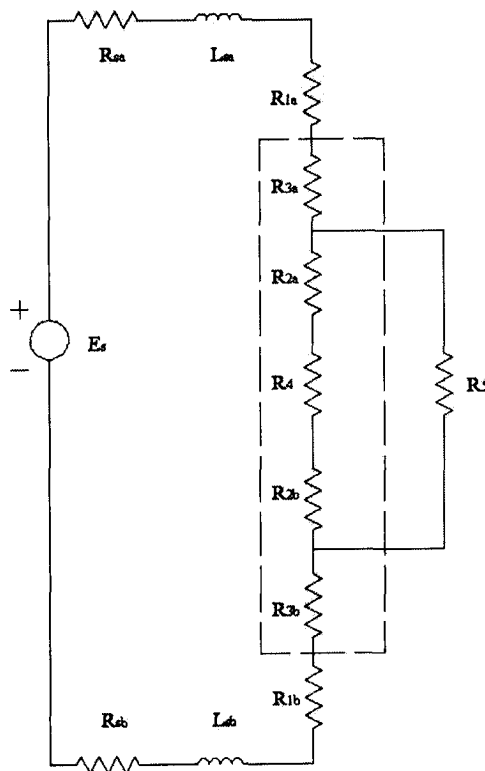


Figure 2.2: Lumped parameter model of the secondary circuit for RSW

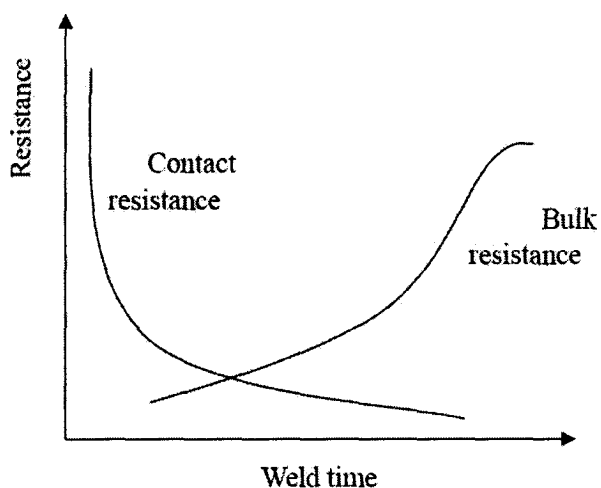


Figure 2.3: Schematic showing the change in resistance during RSW

resistance is an important factor for welding quality in weld of long period. While the contact resistance is a strong function of pressure or force, and also affected by the environment of the contact surface. It will change dramatically as melting commences; therefore the contact resistance is the most important parameter in the beginning few milliseconds in the welding process.

The load resistance attributed to the contributions of the contact resistance and bulk resistance is thus not constant during the process leading to variations in the rate of heating during the weld. Figure 2.3 is schematic showing the change in resistance during resistance spot welding [16].

Based on the above analysis, the following interpretation for the typical shape of the dynamic resistance curve is given. With reference to Figure 2.4, the stages of spot weld formation can be described as follows [17]:

- *Stage I*: The workpieces are brought into contact under the pressure provided by the electrode force. Voltage is applied between the electrodes causing current to flow at the contact points. The resistance between electrodes at this point is

equal to the sum of the bulk resistance of the two workpieces, the two electrode-to-work contact resistance, and the work-to-work contact resistance. Under normal conditions, the initial contact resistance will be very high. Therefore, the initial generation of heat will be concentrated at the surfaces, especially at the the work-to-work contacts. This heat will cause the surface contaminants to break down, resulting in a very sharp drop in resistance.

- *StageII*: Immediately after the breakdown of surface contaminants, metal-to-metal contact exists. However, the surface resistance may still remain relatively high due to the limited area for current flow provided by the asperity contacts. Heating then is concentrated at the work-to-work surface, and temperature in this region and in the bulk materials will increase. As heating progresses, the asperities soften and the contact area increases thus causing resistance to decrease. At the same time increasing temperature result in increasing resistivity, thus providing an opposite effect. Eventually, the increase in contact area will be overcome by the increasing temperature effect, and the total resistance will begin to rise.
- *StageIII*: During this period, the increase in resistivity resulting from increasing temperature dominates the resistance curve.
- *StageIV*: The bulk of the workpieces continue to increase in temperature, thus causing resistivity and resistance to increase. But the heat being generated also cause additional melting to occur at the surfaces, increasing the size of the molten region and the cross-sectional area available for current flow that causes a resistance decrease. Also increased softening will result in some mechanical collapse, shortening the path for current flow and decreasing resistance. Therefore the resistance starts to decrease.

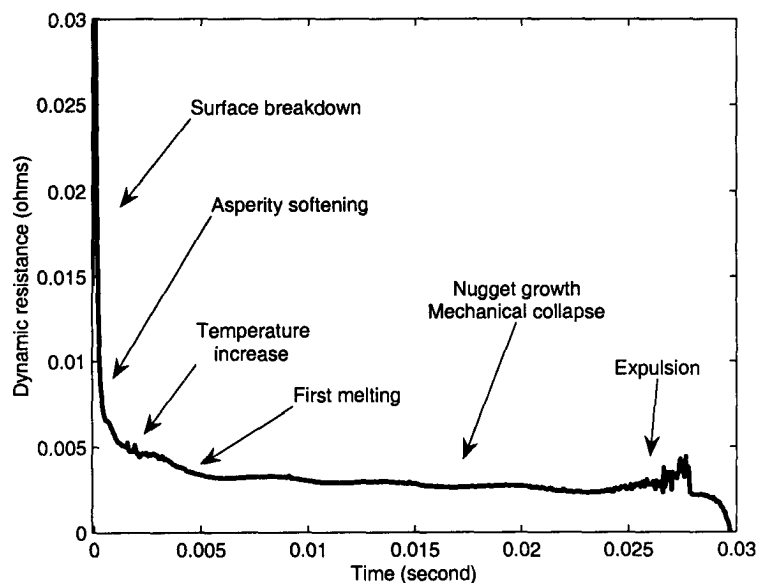


Figure 2.4: Theoretical dynamic resistance curve

- *Stage V*: The growth of the molten nugget and mechanical collapse continue to cause resistance to decrease. If the nugget growth to a size such that it can no longer be contained by the surrounding solid metal under the compressive electrode force, expulsion will occur.

This series of events offers a consistent interpretation of the shape of the dynamic resistance curves observed for spot welding process. Variables expected to cause significant variation in the shape include current level, electrode force, and materials being welded.

It should be noted that with different control modes for the welding power, even if the final Q is kept constant, the heat supplied at intermediary stages will be different. Thus constant voltage, constant current and constant power welds will all have different properties, including weld strength and nugget size despite having identical final Q values.

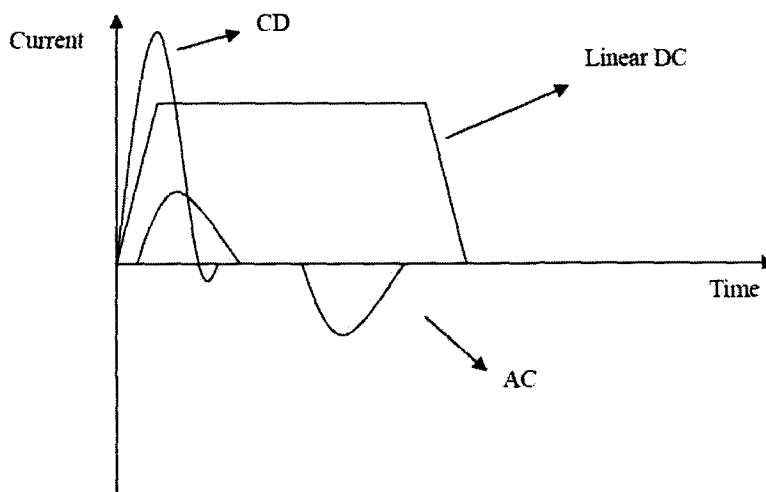


Figure 2.5: Schematic of current waveforms of CD, DC and AC power supplies

2.2.2 Review of Existing RSW Power Supplies

There are different types of power supplies used in RSW [13]:

- Line Frequency AC Power Supply, which provides alternating current (AC) of the same frequency as the input power line;
- Direct Current (linear DC) Power Supply, which provides pure DC weld current through power transistors working in linear range;
- Capacitor Discharge (CD) Power Supply, which provides the weld current by discharging the energy stored in a capacitor bank. Typical AC, CD and DC current waveforms are shown in Figure 2.5

Most large-scale resistance spot welding systems use line frequency AC power supplies [8]. When an AC power supply is used, output current is generally sinusoidal waveform of the same frequency as the input power line current, which is $50/60\text{Hz}$ alternating current AC, and the heat is controlled by changing voltage and switching

off the current for a portion of each cycle. Through the use of silicon-controlled rectifiers, the current is conducted in a controlled manner; therefore the resultant current to the workpieces appears as shown in Figure 2.5.

The original AC power supplies were open loop controls. In order to improve the welding quality and consistency, new AC welding technology that provides closed loop control over weld current has appeared. But it has poor control ability at short cycle times. This type of power supply is normally sensitive to the power line voltage change, which is another limitation of the AC power supply. The advantages of the AC power supply are: reliable, rugged and inexpensive.

A newer technology finding niche application in industry is the mid DC supply. With this approach, standard 50/60Hz AC power is first rectified, converted to a 400 to 2000Hz AC with an inverter, stepped down through a transformer and then rectified again. Control of the amount of power supplied is achieved at the inverter stage. The mid frequency DC (MFDC) power transformer has the identical purpose as with the weld transformer in the traditional AC welder. The major difference lies in the size of the magnetic iron core that transform primary current into secondary current. Since the MFDC transformer relies on the control to provided it with frequency pulses of 400 to 2000Hz instead of the base 50/60Hz, the amount of iron in the core is reduced significantly. This allows the transformer to be placed much closer to the welding tool in some cases hence providing further benefits. The control of power is achieved by control of the inverter. It appears that the MFDC does not cause line disturbances as is the case with the low frequency DC transformer. In fact, there are advantages for the electrical power supply to install MFDC transformers for resistance welding [18]. And it is preferred technology for higher currents associated with welding aluminum.

Downsized welder power supplies are used for small-scale RSW systems (SSRSW). Most SSRSW applications use "closed loop" controlled power supplies including constant current, voltage and power control modes and providing faster speed and smaller time intervals, such as linear DC power supply. Linear DC power supply is also called transistor direct power supply. A linear DC power supply consists of a transformer, an ac-dc rectifier, a capacitor bank and power transistors. The transformer steps down the high voltage from power lines to a lower level welding voltage. Then through the AC/DC rectifier, the AC current has been converted to DC current. And the capacitor bank is used to store the energy. Finally, the controlled transistors act as direct energy source to delivery the pure DC current to weld head and workpieces. This technology has excellent control repeatability, but the restriction to low powers restricts it to thin foils and fine wires [13].

Some of the SSRSW applications also use CD power supplies, which use "open loop" control scheme. CD Power Supply is also called "Stored Energy" power supply [16]. When a CD power supply is used, the energy is provided by a charged capacitor bank and the amount delivered is determined by the amplitude and duration of the current pulse. The heat input can be controlled by varying the voltage on the capacitor bank that changes the amplitude of the current pulse. This kind of energy source exhibits good repeatability of the amount of stored energy, and it is rugged and inexpensive. However, since weld time is dependent on the output pulse width, so the weld time selection is very limited. Variability of weld conductor impedance changes the energy delivered to the weld. Variability of the weld resistance significantly impacts duration of weld and amount of heat dissipated during weld, resulting in variability of final temperature and weld properties. Further, limits on capacitor size limits this approach to small scale spot welding.

A switch mode DC power supply was used in our research. This power supply was used as it provided no restrictions on controller implementations or strategy. Commercial power supplies generally are restricted to applying fixed current or voltage set points and are not easily modifiable. The present power supply is a small scale spot welding supply but can easily be upgraded to a full scale spot welder. The power supply is a pulse width modulated DC-DC converter. Thus its nominal output is given by the duty cycle times the maximum voltage.

2.2.3 Resistance Spot Welding Sequence

The spot-welding process is composed of a series of discrete events that occur over a short period in time as shown in Figure 2.6 [1].

During "squeezing", the electrode move together; the force is applied from pneumatic cylinder and reaches its preset steady state value. The weld force will make the two workpieces contact well and then provide proper faying resistance for the heat generation.

The second step of the RSW is called "welding", when the welding current is conveyed by the electrodes to the workpieces, and generates the energy to melt the parts of workpieces to form the nugget. Real time closed-loop control is applied during this step, which is provided by the welding power supply.

The last step of a RSW welding is "hold", which is also called "cooling time". The purpose of this step is to hold the molten nugget of the workpieces for a certain period of time until it cools down and becomes a stable and solid nugget. The welding force is still employed in this step to hold the joints. To finish, the upper electrode is lifted up allowing the workpieces to be moved away and gets ready to start the next weld.

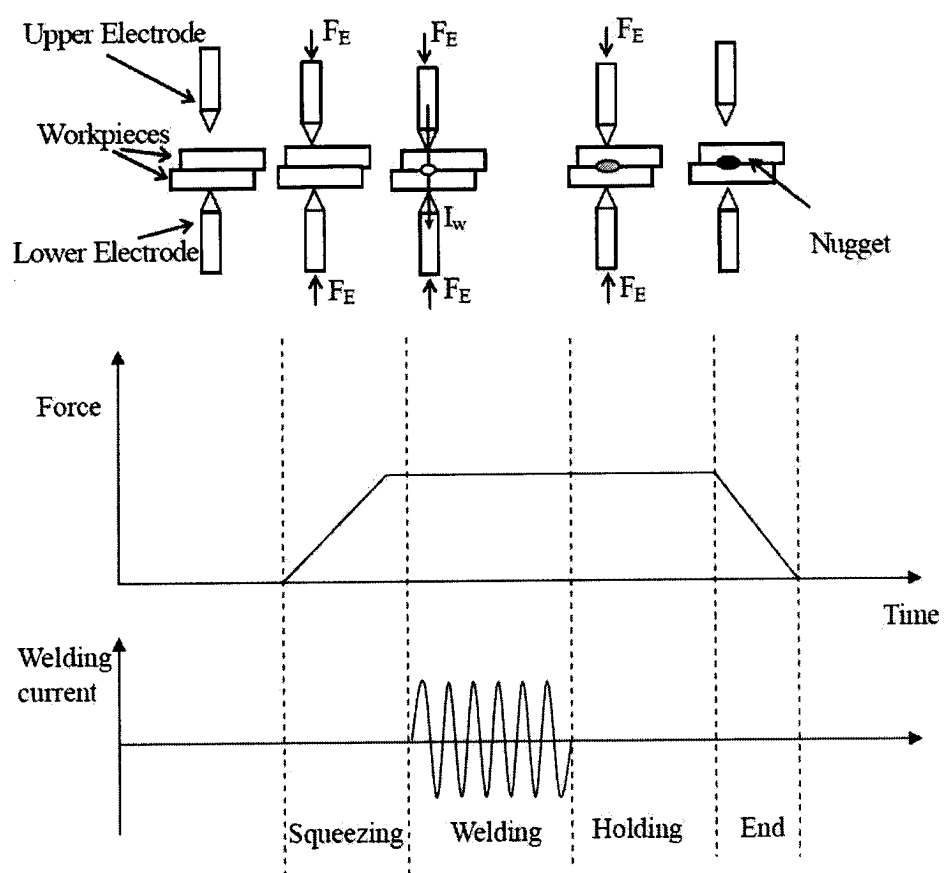


Figure 2.6: The procedure of RSW

It has been indicated that nugget formation and development can be characterized as a function of welding variables (weld time, current and electrode force) by following principle stages [19]:

- initiation of nugget,
- rapid nugget growth,
- steadily decreasing growth,
- weld metal expulsion.

As the contact resistance is strongly influenced by the pressure, electrode force is believed to be a critical factor affecting the process, especially at the early stages in the heating cycle [20]. Higher electrode force usually reduces the contact resistance at the electrode-sheet interface and, hence, would decrease the heat/temperature at the surface and hence may reduce the tendency of expulsion. Therefore, electrode force determines the maximum nugget diameter without expulsion when the electrode geometry is kept constant. And higher electrode force broadened the process window of welding current, which may be because electrode force can increase the onset current for expulsion than it can increase the threshold current to form a weld. However, a large electrode force can lead to excessive surface indentation, which is often undesirable during micro-joining or precision welding.

Welding current is another significant variable affecting nugget formation and growth as the power generated is proportional to the square of welding current as indicated in Equation 2.1. The current range is determined by evaluating the minimum and maximum current levels permissible for required joint properties [21]. A certain level of welding current is generally required to produce adequate heat energy for a

weld with a minimum nugget diameter. However, excess welding current causes void and crack formations.

The effect of welding time can be also observed during the formation of weld nugget. A longer weld time allows more heat to be conducted to the sheet metal. However, longer weld time would increase the softening effect at the heat-affected zone and hence decrease the joint strength when welding cold-worked sheet metal (such as Al sheet) [22].

The weld time, weld current and weld force are the key control variables for regulating the quality of the weld nugget. These variables are strongly cross-coupled and thus any of these parameters may be adjusted to influence the quality of the spot weld produced, within a moderate range of values. The resulting weld may exhibit a few characteristics that often serve as indicators of the weld quality [23].

- *Expulsion*: The most frequently noticed is expulsion. This is a characteristic of over-welding where molten metal is expelled from the weld nugget as a violent shower of sparks. The latest theory of expulsion is that it happens when the force from the nugget due to the internal pressure in a liquid nugget caused by melting, liquid expansion, and other factors exceeds the force from the electrodes [24]. And severe expulsion can reduce the joint strength because of the loss of metal volume. In addition, expulsion has a negative influence on adhesive bonding, if it is used in conjunction with spot welding, by damaging the adhesive layer; therefore, it should be avoided. Expulsion always occurs towards the end of the weld time as a nugget must have overdeveloped in order for this condition to have occurred.
- *Surface expulsion*: This is produced when worn or misaligned electrodes are used. Degradation of the tip of the electrodes increases the resistance of the

interface between the electrode and the workpiece. An increase in this resistance results in a higher proportion of the welding energy being dissipated into this interface causing localized melting to occur at the interface of the workpiece. This molten material may then be released via a similar mechanism to normal expulsion, however, this condition is generally less violent. The high electrode temperatures generated by this condition promote further erosion of the electrodes thus adversely affecting electrode life.

- *Cold weld*: This is a result of severe under-welding where a weld nugget does not form. This is caused by insufficient current or a short weld duration causing insufficient energy to be put into the weld zone.
- *Under-size weld*: This is a spot weld where a nugget has formed; however, the nugget diameter is less than the minimum size specified in the design. The required nugget diameter is dependent on the classification of the spot weld. Both expulsion and undersize weld are often used as visual indicators of a correct welding process.
- *Sparking*: This occurs at the electrode-workpiece interface when the weld current is initiated before electrode set-down. The sparks are generated when the electrodes contact the workpieces resulting in erosion on the electrode surface and may result in the electrodes becoming bonded to the workpiece. Severe sparking can inflict significant damage to electrodes in a single weld and may damage the welding power supply.

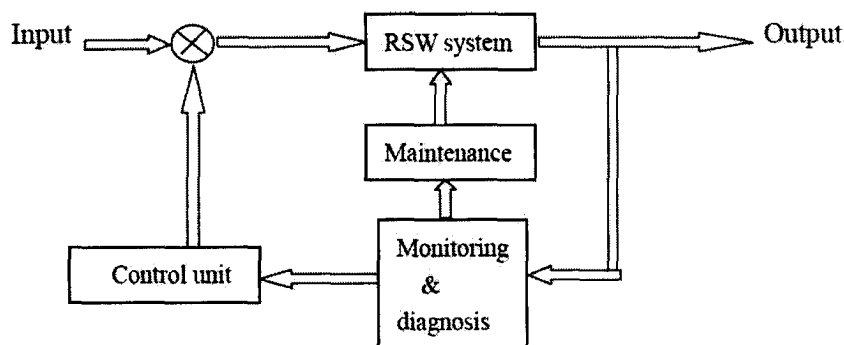


Figure 2.7: Schematic of a typical RSW monitoring and control system

2.2.4 Signals Commonly Monitored during Welding Process

Monitoring a welding process provides useful information on the physical processes involved in welding, and it is a necessary step toward successful control of the process.

A general-purpose RSW monitoring and control system consists of three parts (as shown in Figure 2.7) [24]: a welding system, a monitoring unit and a control unit. The system begins with an input to the welder, usually in the form of a welding schedule specifying welding current or voltage depending on the weld controller, time, and electrode force. The output of the welder is then fed into the monitoring unit, which comprises data acquisition and signal processing. The processed information is then passed on to the control unit. If an action is warranted, the control unit will modify the input and alter the schedules for subsequent welding process. In this section, common signals collected during RSW are discussed, and their use for welding process monitoring is presented. Intuitively, welding voltage and current should be monitored, as they are directly related to joule heating, or the formation of a weld nugget.

Electric Current: Welding current is an important variable to monitor. This variable is considered as the objective of advanced commercial control systems to

keep the heat generation consistent. And some controllers sense only the welding current and signal a fault when the measured value does not fall within prescribed limits. Hence, it is necessary to measure the secondary current of the welding transformer [24]. It is usually measured using either a sensor based on the hall effect or a toroid sensor. Similar to tip voltage, the welding current itself does not represent the input heat either. In order to determine the heat input to a weld, both voltage and current must be measured.

Electrode Tip Voltage: Monitoring the electrode tip voltage can provide very valuable information about the weld process. Although the voltage itself does not directly represent the heat generation or nugget growth, a number of adaptive control units have been developed that shut off the current at some predetermined voltage level [25].

However, the tip voltage can not be measured directly in an AC RSW circuit. So it is not common to monitor this signal. Since the voltage probes must span the thickness of workpieces, a loop will exist in the voltage measuring circuit, and an inductive voltage proportional to the derivative of the secondary current will be introduced [1]. It is well known that to minimize the inductive noise, one can use twist pairs to reduce the area of the wire loop. However, because of the large currents involved, the constraints on placing the measuring wires to allow access to the workpieces, the induced voltages are inevitably larger than the actual tip voltage [26]. Thus, in practice with AC welding supplies, voltage is measured only once per half cycle at the peak current when the induced voltage is zero. For switch mode DC supplies, the bandwidth of current sensing must be kept well below the switching speed of the DC supply.

Dynamic Resistance: Dynamic resistance is a measure of the electrical resistance change during welding. Resistance is found by dividing the measured voltage

by the current. Hence all of the same difficulties for measuring tip voltage apply to finding the resistance. Further for AC welding, no resistance can be determined for those periods where the weld current is zero. Dynamic resistance has been shown to have a good correlation to the nugget growth and is currently receiving more attention. The phenomena occurring during spot weld formation can be understood through analysis of dynamic resistance curves. See Figure 2.4 showing the typical dynamic resistance for resistance spot welding process. After an initial drop, it too rises to a peak in the first portion of the weld cycle, dropping off later in the cycle. If expulsion occurs during a spot weld, it also is readily detected from a continuous measurement of this parameter. The main indicator for expulsion is the instantaneous drop in the resistance.

For assuring quality welds, the electrical current, tip voltage and dynamic resistance signals have been the most used in monitoring and controlling the welding process.

2.3 Small Scale RSW and Micro-RSW

Large scale resistance spot welding is well over 100 years old and represents a mature joining process [27]. There has been ample time for materials to become standardized as to alloy types, plating, and thickness. These factors have been driven the creation of welding tables that clearly define the large scale resistance spot welding process.

In recent years there is an increasing need for very thin metal welding in applications. Extensive research and development work has penetrated in the area of small and micro-scale resistance spot welding. Small and micro-scale resistance spot welding is being fueled by the explosion to make everything smaller, from automotive electronics, to telecommunications components and medical products.

The monitoring and control of the small and micro scale resistance spot welding process is less commonly addressed in the literature than the large scale resistance spot welding process although there are some significant differences between the two [28]. Since the workpiece in the small and micro scale process is relatively thin, electrode displacement monitoring requires higher resolution and is much more difficult than for the large scale process. The small and micro scale process is relatively fast, the welding time being typically tens of milliseconds instead of hundreds of milliseconds. The much smaller currents permit the use of higher bandwidth high frequency inverter or linear power supplies rather than low-to-medium frequency inverter used in the large scale process. Also the small and micro scale process uses much smaller electrode force.

According to the thickness of the joint metal sheet the RSW can be classified into three classes, large scale RSW (LSRSW), small scale RSW (SSRSW) and micro-RSW. The LSRSW usually deals with metal sheets with a thickness above 0.41 to 1.57mm, while the Micro-RSW handles work pieces thinner than 0.125mm, and the SSRSW works on the workpieces with a thickness between the other two classes. Table 2.2 presents a comparison of the three RSW classes [8].

Table 2.1: Classification of welding processes

Group	Welding process	Letter designation
Arc welding	Carbon Arc	CAW
	Flux Cored Arc	FCAW
	Gas Metal Arc	GMAW
	Gas Tungsten Arc	GTAW
	Plasma Arc	PAW
	Shielded Metal Arc	SMAW
Brazing	Diffusion Brazing	DFB
	Dip Brazing	DB
	Furnace Brazing	FB
	Induction Brazing	IB
	Resistance Brazing	RB
	Torch Brazing	TB
Oxyfuel Gas Welding	Oxyacetylene Welding	OAW
	Oxyhydrogen Welding	OHW
	Pressure Gas Welding	PGW
Resistance Welding	Flash Welding	FW
	High Frequency Resistance	HFRW
	Percussion Welding	PEW
	Projection Welding	PRW
	Resistance-Seam Welding	PSEW
	Resistance-Spot Welding	RSW
	Upset Welding	UW
Solid State Welding	Cold Welding	CW
	Diffusion Welding	DFW
	Explosion Welding	EXW
	Friction Welding	FRW
	Hot Pressure Welding	HPW
	Ultrasonic Welding	USW
Soldering	Dip Soldering	DS
	Furnace Soldering	FS
	Induction Soldering	IS
	Infrared Soldering	IRS
	Iron Soldering	INS
	Resistance Sodering	RS

Table 2.2: Comparison between LSRSW, SSRSW and Micro-RSW

Groups	Thickness(mm)	Typical materials	Common applications
LSRSW	0.41 – 1.57	Cold Roll Steel	appliances
		Stainless steel	steel furniture
SSRSW	0.125 – 0.51	Brass Alloys	electronic terminals
		Copper	electronic terminals
		Copper Alloys	bi-metal components
		Inconel	aircraft components
		Molybdenum	auto headlamps
		Nichrome	bi-metal sensors
		Silver Alloys	relay contacts
		Stainless Steel	small surgical instruments
		Tungsten	auto headlamps
micro-RSW	0.0125 – 0.125	Copper	electronic circuit connections
		Gold	electronic circuit connections
		Nickel	electronic circuit connections
		Nitinol	medical guide wires, stents
		Platinum	electronic circuit connections
		Stainless Steel	micro-cutting instruments

Chapter 3

Control Strategy Design for Resistance Spot Welding

In this chapter, a new power supply strategy to improve the consistency of resistance spot welding for every spot weld is presented. The generic power control mode has been discussed and implemented for the resistance spot welding process. The three control modes, voltage control, current control and power control modes can be seen as three special points in this generic power control mode. A comparison of resulting voltage, current and power curves for constant power, constant current and constant voltage control schemes will be discussed in the last section of this chapter.

3.1 Definition of the Geometric Mean

The geometric mean is an alternative means of finding average value which is more appropriate when numbers vary over wide ranges or have different scales. It is similar to the arithmetic mean, except that instead of adding the set of numbers and then dividing the sum by the count of numbers in the set, n , the numbers are multiplied and then the n th root of the resulting product is taken. The geometric mean of a data set $[a_1, a_2, a_3, \dots, a_n]$ is given by:

$$\prod_{i=1}^n (a_i)^{1/n} = \sqrt[n]{a_1 a_2 \dots a_n} \quad (3.1)$$

Thus the geometric mean of voltage and current is $(VI)^{1/2}$, i.e. the square root of the power. And in statistic, given a set of data $X = x_1, x_2 \dots x_n$, corresponding weights $W = w_1, w_2 \dots w_n$, the weighted geometric mean is calculated as:

$$\bar{x} = \left(\prod_{i=1}^n x_i^{w_i} \right)^{1/\sum_{i=1}^n w_i} \quad (3.2)$$

In fact, power or some other weighted average of current and voltage can be used to improve weld consistency. Based on this point, a weighted geometric mean of variables V and I would be given by $V^{1-\alpha}I^\alpha$ where $0 \leq \alpha \leq 1$ is the weighting. We propose that any weighted geometric mean of voltage and current is a viable control variable and that this approach unifies the existing constant current ($\alpha = 1$), constant power $\alpha = \frac{1}{2}$ and constant voltage $\alpha = 0$ strategies.

3.2 Control Strategy Design

It should be noted that this weighted mean of voltage and current is not, in general, a physically meaningful quantity and as thus has no natural units associated with it. Thus, a scaling constant K , which will be a function of α should be incorporated in the calculation to compensate for unit choice. Thus our control power variable will be designated as

$$P_g(\alpha) = K(\alpha)V^{1-\alpha}I^\alpha \quad (3.3)$$

For this thesis, $K(\alpha)$ is taken to be 1 when V has units of *volts* and I has units of *amps*.

Based on the definition of this control variable, a generic power control mode was designed. Figure 3.1 gives the block diagram of this generic weld power control

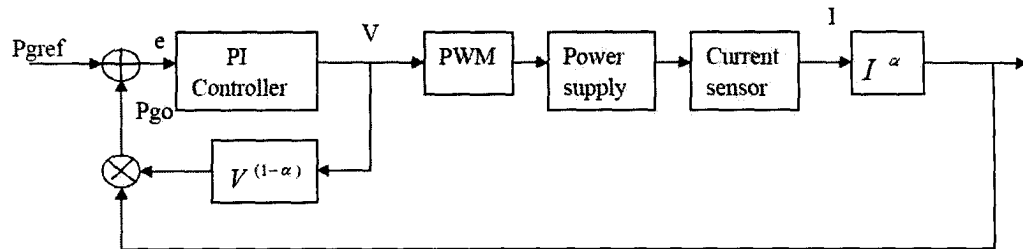


Figure 3.1: Generic power control mode

scheme. The desired output power is given as a power reference (P_{gref}). The system feedback is the power (P_{go}), which is the product of the voltage and current ($P_{go} = V^{1-\alpha} I^\alpha$). And in this study, the voltage setting V was specified as the duty cycle of the power supply and is analogous to firing angle for a traditional AC welder, while the output current (I) was measured through the current sensor. According to the error signal ($e = P_{gref} - P_{go}$), the PI controller changes the PWM duty cycle to regulate the output power.

Having defined this class of weld power controllers characterized by the parameter α , it remains to determine the α that produces the best weld. It is expected that this value will be strongly dependent on the geometry of the weld parts and characteristics of the power supply used.

One approach to find the best α is to define the best as the most consistent, i.e. the one that has least variance in the heat delivered. This idea generates a simple optimization problem based on the model of Figure 2.2. During weld setup, when the basic settings for weld power, weld force and weld time are determined, additional data could be collected that would allow the weld engineer to identify both nominal values for the resistances, as well as measures of the uncertainty or variability of these values. This could be as simple as maximum and minimum values, or variances. With this information, a corresponding uncertainty of Q as a function of α could be calculated.

Table 3.1: The generic control and other control modes

α	$P_g = V^{1-\alpha} \times I^\alpha$	Generic power control
0	$P_g = V$	Constant voltage control
0.5	$P_g = \sqrt{V} \times I$	Constant power control
1	$P_g = I$	Constant current control

The α that minimizes this variability would then be a reasonable choice for use in a production environment.

An alternative strategy would be to empirically determine the weighting that produces the most consistent nugget size or strength. In the following chapters we pursue this strategy for one specific weld geometry and power supply to show the potential for this approach.

3.3 Open Loop Voltage Control Mode

The generic power control scheme covers different control modes with the corresponding α values. The constant voltage control, current control and power control modes can be seen as special points in this mode. Table 3.1 gives the relationship between the generic power control mode and the other control modes.

The open loop voltage control mode ($\alpha = 0$) is to control the PWM duty cycle D as constant to achieve the theoretical constant output voltage. Note that when α is set equal to zero, the control loop around the welder is opened, and the PI controller is no longer necessary. Figure 3.2 shows the diagram of the open-loop voltage control mode.

Under the open loop voltage control mode, the desired output voltage is given as a voltage reference V_{ref} . And the duty cycle D is calculated as the ratio of desired

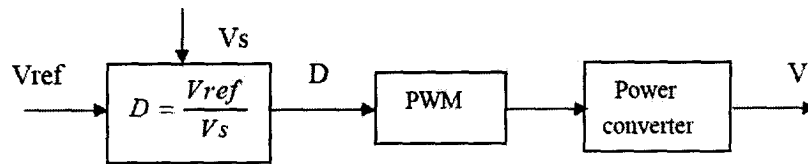


Figure 3.2: Block diagram of open loop voltage control mode

output voltage by the source voltage. Then the calculated duty cycle D is implemented to generate the PWM signals, which control the power converter to produce the output voltage V to the welder. The output voltage V equals to the product of the source voltage and the PWM duty cycle. Because source voltage is a constant, the output voltage is only determined by the duty cycle.

3.4 Comparison for Different Control Schemes

Different control modes have different output effects. Figure 3.3-3.5 illustrate the difference between the three standard control modes in the output variables, where V stands for the output voltage, I the output current and P the output power. As shown in the figures, 100% voltage set point is applied for first $0.4ms$. This done to allow basic PI controller with no modifications to be employed. Otherwise, the PI controller would be significantly in saturation and nonlinear anti-windup strategies would be required.

For the open loop voltage control, the output voltage set point is controlled directly to keep constant. While under the closed loop current control mode, the welding current is regulated as constant, and the duty cycle is adjusted according to load resistance, and the power changes accordingly. In the constant power control scheme, the voltage is adjusted to keep the power constant. Consequently, the current changes as well.

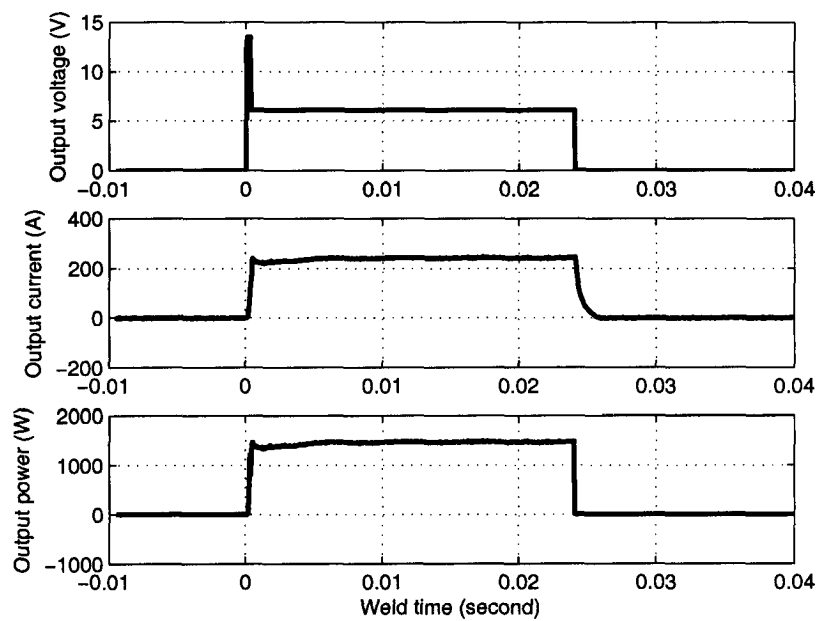


Figure 3.3: Experimental results for the open loop voltage control mode

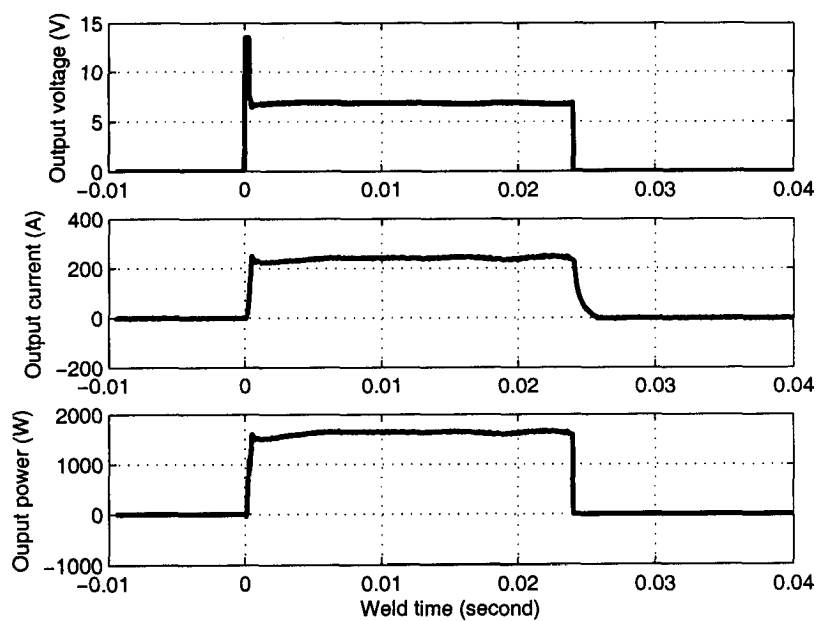


Figure 3.4: Experimental results for the pure current control mode

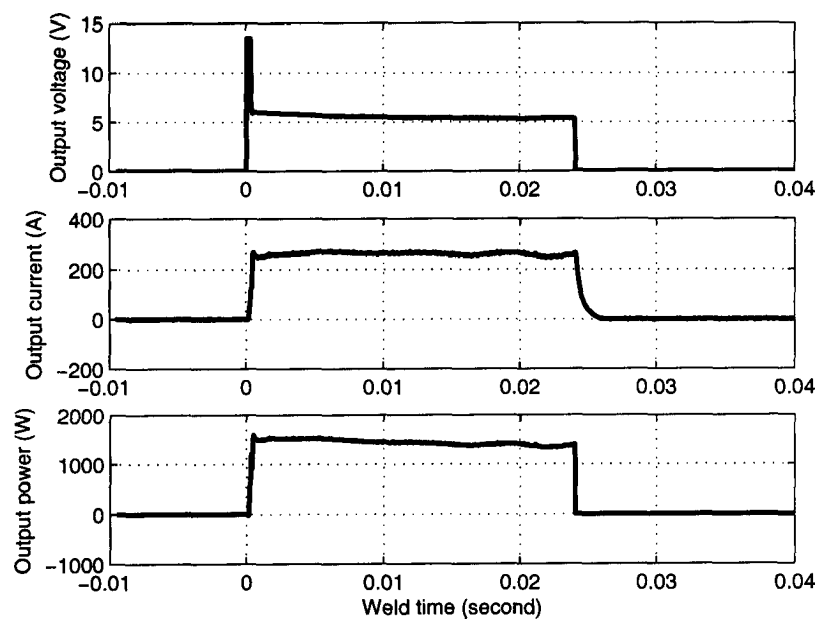


Figure 3.5: Experimental results for the constant power control mode

Chapter 4

Spot Welding System Description

In this chapter, a small scale resistance spot welding system for our experiments has been presented, which uses high frequency switching and Dspace control system techniques to convert the power from a 12V battery to power the welder system. (Note the open circuit voltage of a 12V battery is in fact 13.5V) The technical requirements are discussed first, then the system description, followed by the detailed description of the individual hardware sections including the power section, control electronics section and Dspace control system.

4.1 Technical Requirement

In this study, an Unitek Peco Model 80 Series Weld Head has been chosen as the test device. Table 4.1 gives a summary of the technical requirements for the SSRSW power supply [13].

Table 4.1: Technical requirements

Feature	Minimum	Maximum
Weld force (lb)	0.25	20
Welding current (amps)	50	1000
Electrode tip voltage (volt)	0.1	5
Welding time length (millisecond)	10	99

The individual parameter will be determined according to specific welding conditions, like material, thickness, force, etc. According to the model of weld head chosen, the welding force can be adjusted within a range of 0.25 to 20lbs. The setting of load current depends mainly on the material and dimension of the workpieces, the geometry of electrodes, and the welding force. The material used in this research is 0.152mm gauge stainless steel. Electrode tip voltage is another parameter for control of the welding qualities. The range of tip voltages for SSRSW can be estimated based on the required welding current, generally from hundreds of millivolts to several volts. The welding quality is mainly affected by the setting of these parameters that are commonly monitored during welding.

4.2 System Description

The resistance spot welder system which consists of three major sections: the power section, the control electronics and the Dspace control system. The weld power supply was designed and built by the University of Western Ontario and was described in [13] with minor modifications. Figure 4.1 gives the system block diagram.

In the power section, the MOSFETs are used as the switching components to regulate the output. And the control electronics section includes the driver circuit for the MOSFETs, the sensing circuit for the output current, and other electronics circuit for the control purpose. Based on the given reference and feedback signals from the sensing circuits, the control schemes are implemented to provide the PWM signal to drive the MOSFETs in the power section.

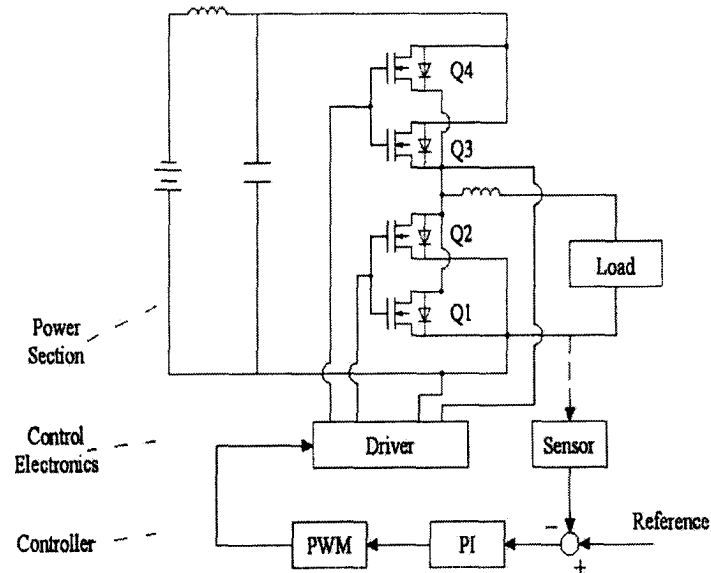


Figure 4.1: Resistance spot welding system

4.2.1 Power Section

The power supply is a pulse width modulated DC-DC converter. Thus its nominal output is given by the duty cycle times the maximum voltage of 13.5V. Power MOSFETs are used as the switching components. Power capacitors are used to compensate for the induction of the battery cables. An output inductor is used to filter the output current.

4.2.2 Control Electronics

The control electronics section is used to drive the MOSFETs according to the PWM signals, and measure the load current from the sensing circuit.

The driver circuit takes the logic level PWM signal, outputs four gate signals to drive the high and low side MOSFETs Q1, Q2 and Q3, Q4.

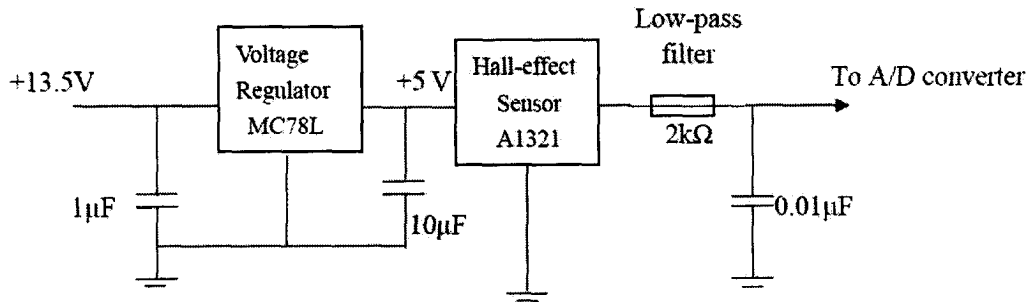


Figure 4.2: Sensing circuit for output current

The task of the sensing circuit is to transform the measured signals into appropriate voltage signals for measuring with an analogy to digital converter. The load current signal is measured to support implementing the control schemes.

Figure 4.2 shows the voltage regulator and current sensing circuit. The voltage regulator MC78L is applied to convert the input power from the 13.5V battery to an appropriate output voltage of 5V to power various other electronic chips.

The A1321 Hall-effect sensor and a magnetic core are used to measure the magnetic field induced by the load current. Figure 4.3 shows the mechanic structure of the current sensing circuit. The sensor transforms the magnetic field into a proportional voltage signal with a resolution of 5 mV/Gauss. Then the voltage signal goes through a low-pass filter to feed the A/D converter in the Dspace system. The induced noise can be eliminated by using the low-pass filter at a cutoff frequency of 50kHz. Through experimental calibration, the scaling of the current sensor is obtained as 0.4 A/mV.

4.2.3 Dspace Control System

The Dspace system based on the DS1104 R&D controller board is the central control unit of the system, which comprises hardware and software.

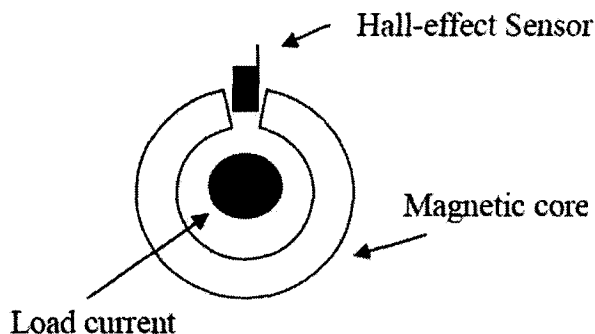


Figure 4.3: Mechanic structure of the current sensing circuit

The hardware DS1104 R&D controller board is a standard board that can be plugged into a PCI slot of a PC. The DS1104 is specifically designed for the development of high-speed multi-variable digital controllers and real time simulations in various field. It is a complete real time control system based on a 603 PowerPC floating point processor running at 250MHz. For advanced I/O purposes, the board includes a slave-DSP subsystem based on the TMS320F240 DSP micro-controller. The DS1104 R&D controller board is a single board system. The hardware package contains one CP1104 connector panel that provides easy-to-use connections between the board and devices. In addition to the CP1104, the CLP1104 connector/LED panel provides an array of LEDs indicating the states of the digital signals.

The Dspace software, such as the implementation and the experiment software, comes on CD-ROM and has to be installed first. And it does the job of signal processing. After installing the Dspace software, the real time hardware is managed by the Platform Manager integrated in ControlDesk software.

Based on the given reference and feedback signals, the Dspace control system implements the control schemes and provides the PWM signal to drive the MOSFETs in the power section.

Chapter 5

Application of Strategy to Welding

0.152mm Gauge Stainless Steel

This chapter demonstrates the benefits that can accrue by replacing constant current control by constant weighted mean of current and voltage control. For this purpose, a series of welds were conducted and the variance of the nugget diameter and tensile strength was measured for the 11 values of α from 0 to 1 by 0.1 increments.

The basics steps in this procedure are [29]:

- Lobe test to determine basic operating variables, i.e weld time, force, and power.
- Tune PI controller gains for each α .
- Identify set points for each α . For valid comparison of the variances of nugget size, it is important that the mean nugget size is held constant. As discussed earlier, the heat input during resistance spot welding is a function of the resistance. Further, the trajectory of the resistance is a function of the control strategy. See Figure 5.1 comparing typical time trajectory of the resistance for constant current and constant voltage welds. Even, if set points could be determined that delivered identical heats, they would not be expected to produce identical welds. (Note that the initial resistance is approximately 270*milliohms* which is consistent with static resistance measurement.)

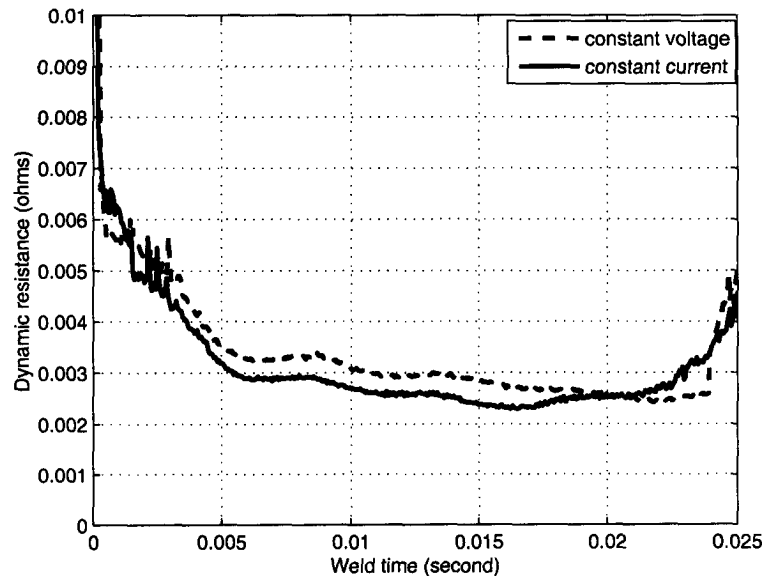


Figure 5.1: Typical resistance under voltage control and current control

- Perform a series of welds for each α and measure mean and variance for nugget diameter and tensile strength.

5.1 Experimental Setup

The experimental setup includes a small scale resistance spot welding (SSRSW) head from Unitek Peco Model 80, electrical current sensor, the developed DC power supply, a data acquisition system and a PC computer. Figure 5.2 shows the block diagram of the setup [13].

A Model CP cable foot pedal is used to apply electrode force after two overlapped coupons are manually placed between the opposing electrodes. The Model CP cable pedal pivots under the heel for optimum force control. It is equipped with an adjustable down-stop which prevents the application of excess force. It is rated

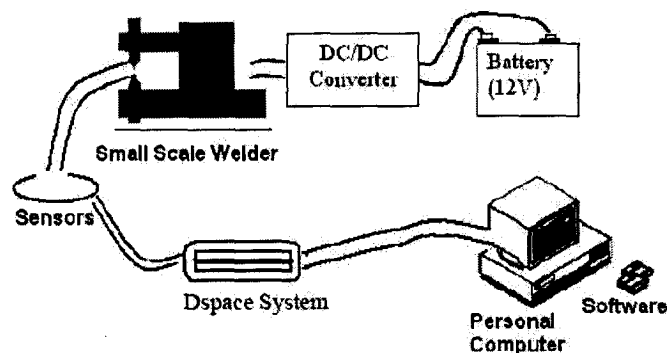


Figure 5.2: Block diagram of experimental set-up

at 25 pounds, and can be used with Unitek Peco Model 80 weld head. When the force applied by the pedal reaches the preset value, the welding current is generated through the electrodes and the workpieces by the DC power supply.

A current sensor is used to measure the welding current transmitted to the PC computer through the data acquisition system. The data acquisition system, including a connector panel (part # CP1104), a DS1104 controller board and the software, is a Single-Board Simulator from DSpace Inc. The connector panel samples the measured signals, and the DS1104 controller board is inserted into the computer and communicates between the PC computer and the connector panel. The software does the job of signal processing.

The electrodes used in the test are ES0402-RWMA2 - (COPPER CHROMIUM ALLOY - 83B Rockwell hardness, 85% conductivity), which are widely used for welding of steels, nickel alloys and other high resistance materials. The dimensions are $1/8$ -inch diameter, $5/4$ -inch long. And the tip electrode diameter is $1/16$ -inch. The whole welding process is semi-automatically controlled. The weld force is applied to squeeze the upper electrode to the lower electrode.

The material being welded was 2 identical 0.152mm gauge stainless steel coupons with dimensions of $40\text{mm} \times 10\text{mm}$. For measuring the weld strength, the setup

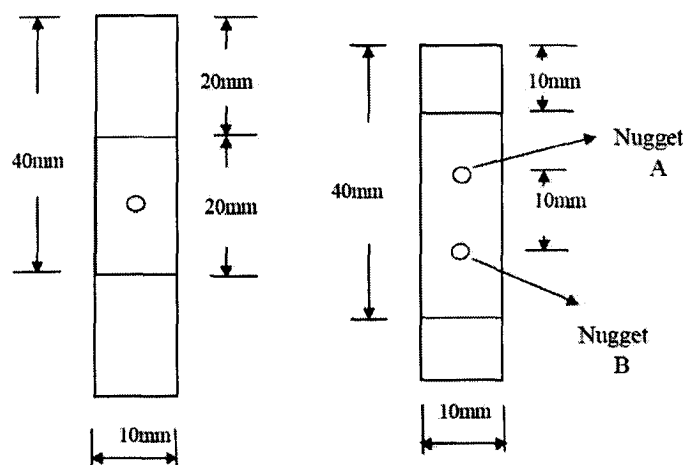


Figure 5.3: (a) Tensile test sample (b) peel test sample

coupons should be assembled to form a tensile shear type geometry test sample with the overlap area being half coupon length. Figure 5.3 shows the welding samples for measuring the weld strength and nugget diameter separately. A single spot weld should be placed in the center of the overlap area of a coupon pair sample. When welding set-up samples the sample orientation with respect to the welding machine throat is to be kept constant. A mechanical test, called tensile test, is commonly used in determining the weld strength.

For measuring the nugget diameter, the overlap area of the assembled test sample should be three-quarters of the coupon length. Two adjacent spot welds should be placed in the overlap area. when welding samples, the second weld nugget (B) should be marked to differentiate from the first one (A). The peel test is used to measure the nugget diameter. Both the tensile test and peel test will be introduced in the below section.

5.2 Lobe Test for Open Loop Voltage Control Mode

5.2.1 Weld Lobe

"Weld Lobe" is used to describe the condition of weld current, force and time, which allows satisfactory welds to be performed. The weld lobe is usually determined through "Lobe Tests". Lobe testing is an effective aspect of weldability study. Such testing is either for obtaining quantitative measures of a weld's strength which generally refers to the capability of standing load, or for revealing important weld characteristics, such as weld button diameter [24].

The objective of a lobe test is to either obtain a quantitative measure or get a qualitative sense of weld quality, the following information is usually collected during a test:

- *Peak load*: The maximum force measured during testing, as illustrated in Figure 5.4 for tensile test. As the most commonly monitored quality index, weld strength has been, in many cases, the sole measure of weld quality.
- *Failure mode*: This is a qualitative measure of weld quality. such as the peel test (Figure 5.5), to see if there is a weld button pullout, interface or weld failure.
- *Weld nugget diameter*: It is easily measured during the test. And the nugget diameter is a substitute as it is believed to correlated to the weld strength.

In this section, testing procedures and measurement are discussed. Details is given for commonly performed tests.

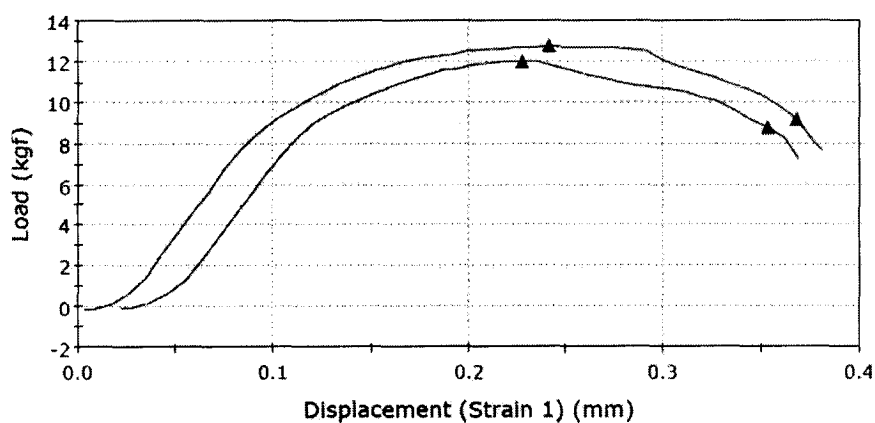


Figure 5.4: Tensile test for measuring weld strength

5.2.2 Tensile Test

For welding the stainless steel coupons, the weld strength can be measured to evaluate the weld quality. A mechanical test, called tensile test, is commonly used in determining the weld strength because of its simplicity in specimen fabrication and testing. In this test, two strips of metal are lapped together and joined by a single weld to obtain a test specimen as shown in Figure 5.3. Then the specimen is pulled in tension to destruction on a standard testing machine. In this study, an Instron 5548 Universal Tensile Tester was used to do the tensile test and the cross-head speed was $10\text{mm}/\text{min}$. Figure 5.4 shows the tensile test curves of two samples. The maximum force should be recorded as weld strength, which has the unit of kgf the same as N .

5.2.3 Peel Test

In fact, the nugget diameter has been indicated as an important quality index because of its correlation to the weld strength. So another simple test for measuring the nugget size is called peel test (Figure 5.5) [13]. When welding samples, the second

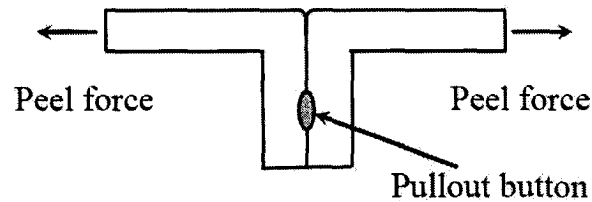


Figure 5.5: Peel test for measuring nugget diameter

weld nugget (B) should be marked as shown in Figure 5.3. In the peel test, the sheets are first separated on one end of a lap joint, and one sheet is rolled up by the roller while the other is gripped. As the roller rolls over the weld, half of the workpiece is torn off at the weld and a weld (A) button is left. With continued peeling, the whole workpiece is torn off and another weld (B) button is left. The nugget size can be estimated and recorded as a parameter for welding quality by measuring the diameter of pullout button (B). If the button shape is irregular, the button diameter is determined by taking an average of the maximum and minimum dimensions.

Various failure modes can usually be observed during the peel testing of welded joints, namely:

- (a) interface failure,
- (b) weld failure, and
- (c) button pullout as shown in Figure 5.6 [22].

Interface failure is due to lack of bonding or only weak bonding between sheets. Once a weld nugget formed, joints generally failed through the nugget when the nugget diameter is small or by a button pullout when it is above a certain size, which is called weld failure or button pullout. The failure modes usually serve as a rough indicator of whether a specimen size is adequate.

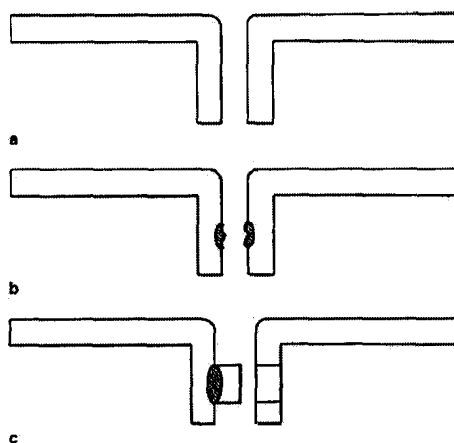


Figure 5.6: Schematic showing joint failure modes during peel test

5.2.4 Lobe Test for Open Loop Voltage Control Mode

Practice of controlling a welding process is made using selected welding parameters, including force, current, voltage and time. Such selection is usually done using a so-called lobe curve, as shown in Figure 5.7 [30].

The lobe curve has been used for many years to characterize a weldability during resistance spot welding. At a fixed force level, a lobe diagram divides the current/voltage-time domain into three regimes in terms of weld quality: undersized or no weld, acceptable weld, and expulsion. For a given material and welder setup, weld lobes are usually developed in a lab environment and then a welding schedule (the settings of welding parameters) is chosen for production based on the weld lobes.

A lobe diagram basically contains two boundaries for minimum acceptable welds and expulsion. The minimum current/voltage at particular welding time corresponds to the acceptable welds meeting the minimum requirements, usually in terms of weld sizes. The minimum acceptable weld sizes depend on the standards used. The maximum current/voltage corresponds to the occurrence of expulsion. Occasionally, a current/voltage corresponding to a nominal weld size is also plotted in a lobe diagram as

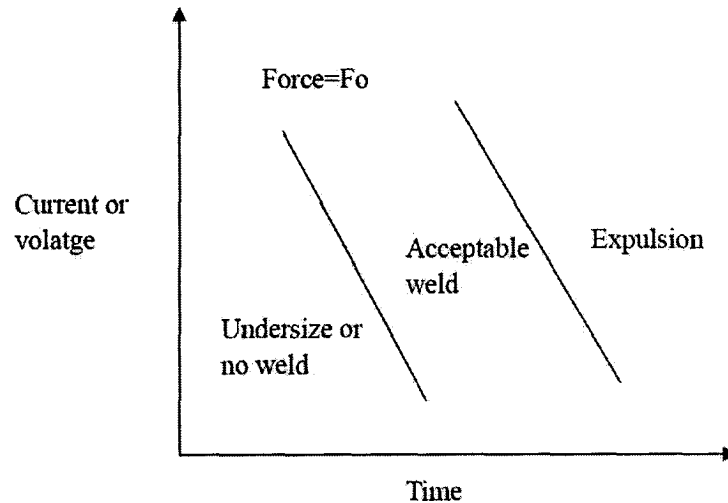


Figure 5.7: A weld lobe diagram

a reference for weld current/voltage selection. The difference between the maximum and minimum current/voltage is the window of operation or current/voltage range.

Once the lobe curve is known, characterization of the dynamic electrical measurement can be made at critical areas on the curve. Such critical areas are:

- around the lower limit line,
- at expulsion,
- within the acceptable region.

In this study, both the peel test and tensile test were conducted to find an appropriate nominal power setting, weld time and electrode forces under open loop voltage control. Power setting was specified as the duty cycle of the power supply and is analogous to firing angle for a traditional AC welder.

- Forces used in the weld lobe study were {1.5, 2, 3, 4} pounds,
- weld times were {12, 15, 20, 23, 25, 26, 28, 30}ms,

- and duty cycles were {40, 45, 50} percent.

20 experiments (10 for nugget diameter measurement and 10 for weld strength measurement) were done at each set of operating conditions. As a result of this test an operating point of (45% duty cycle, 24ms weld time and 1.5lb weld force) was determined from a lobe curve. (see analysis section in the next chapter). All remaining welds were performed with 1.5lb weld force with duration of 24ms.

5.3 Step Test for Constant Current Control Mode

In order to implement the other weld power supply control modes, PI controllers needed to be tuned for each α values. In order to achieve this, a simulink model needed to be built. In this simulink model, the welder system can be simplified as a transfer function from step test method [31].

The step test is a simple test based on a step response for a stable system. It is carried out in the following way. A constant input is chosen. A stable system will then reach an equilibrium. The input is then changed rapidly to a new level and the output is recorded. A simple model of the form:

$$G_{w,v}(s) = \frac{Ke^{sT_d}}{\tau s + 1} \quad (5.1)$$

can easily be fitted to the data. A step test is illustrated in Figure 5.8.

Assume that the input changes with Δu and that the corresponding change in the steady state output is Δy . An estimate of the steady-state gain is give by:

$$K = \frac{\delta y}{\delta u} \quad (5.2)$$

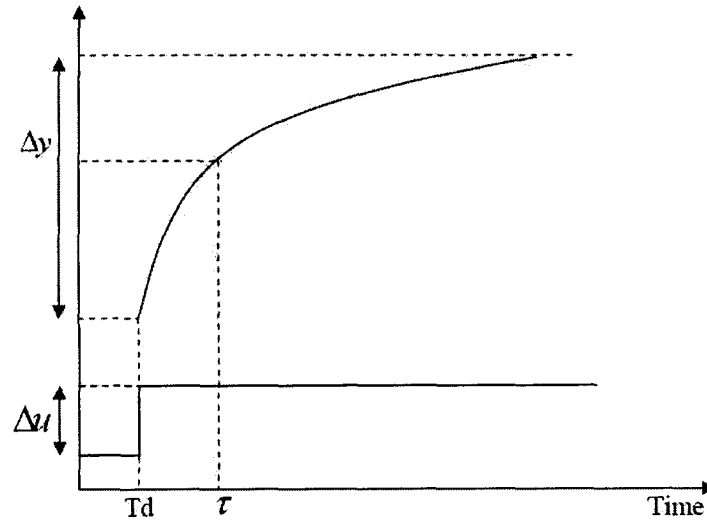


Figure 5.8: Step test input and output

and T_d is the first moment after the output has changed and the time constant

$$\arg_{\tau}\{y(\tau - T_d) = e^{-1}(\Delta y + y(T_d))\} \quad (5.3)$$

Followed the above way, to achieve the transfer function for the welder system in this study, 20 welds were performed with duty cycle set to 40% at the first 14.5ms of the weld and then decreased to 34% until 19.5ms. The resulting currents were recorded and then averaged and fit to a first order with dead time model

$$\frac{\delta I}{\delta D} = \frac{K e^{sT_d}}{\tau s + 1} \quad (5.4)$$

where δI is the difference in current from value at 15ms, δD is difference in duty cycle from 40%,

$$K = (I(40) - I(34))/6 \quad (5.5)$$

and T_d is the first moment after 40% duty cycle that current has changed and the

time constant

$$\arg_{\tau}\{I(\tau - T_d) = e^{-1}(I(40) - I(34)) + I(40)\} \quad (5.6)$$

Figure 5.9 shows the plot of step test result. A simulink model given in Figure 5.10 was then built, and a Proportional-Integral controller (PI controller) was implemented.

The proportional-integral controller (PI controller) is a generic control loop feedback mechanism widely used in industrial control systems [32, 33]. A PI controller attempts to correct the error between a measured process variable and a desired set point by calculating and then outputting a corrective action that can adjust the process accordingly.

The PI controller calculation (algorithm) involves two separate parameters; the Proportional and the Integral values. The proportional term makes a change to the output that is proportional to the current error value. The proportional response can be adjusted by multiplying the error by a constant K_P , called the proportional gain. A high proportional gain results in a large change in the output for a given change in the error. If the proportional gain is too high, the system can become unstable. In contrast, a small gain results in a small output response to a large input error, and a less responsive (or sensitive) controller. If the proportional gain is too low, the control action may be too small when responding to system disturbances.

The contribution from the integral term is proportional to both the magnitude of the error and the duration of the error. Summing the instantaneous error over time (integrating the error) gives the accumulated offset that should have been corrected previously. The accumulated error is then multiplied by the integral gain and added to the controller output. The magnitude of the contribution of the integral term to the overall control action is determined by the integral gain K_I . The integral term (when

added to the proportional term) accelerates the movement of the process towards set point and eliminates the residual steady-state error that occurs with a proportional only controller. However, since the integral term is responding to accumulated errors from the past, it can cause the present value to overshoot the set point value.

By "tuning" the two constants in the PI controller algorithm the PI can provide control action designed for specific process requirements. The response of the controller can be described in terms of the responsiveness of the controller to an error, the degree to which the controller overshoots the set point and the degree of system oscillation. Note that the use of the PI algorithm for control does not guarantee optimal control of the system or system stability.

Tuning a control loop is the adjustment of its control parameters to the optimum values for the desired control response. The desired behavior on a process change or set point change varies depending on the application.

In this study, the PI controller was tuned manually. As the overshoot for our system can not be eliminated to zero, it was specified within the range between 6% and 9% with maximizing the speed of response.

By using the simulink model (Figure 5.9) with $\alpha = 1$ (pure current control), a PI controller, that gave 7.9% overshoot with fastest rise time was then built. (see analysis section in the next chapter).

The resulting gains were designated K_p and K_I . This was then repeated for the 10 α values evenly spaced between 0.1 and 1 inclusive. To ease this repeated design, initial guesses for the PI controller parameters were chosen as

$$K_p(\alpha) = \alpha K_p \quad (5.7)$$

$$K_I(\alpha) = \alpha K_I \quad (5.8)$$

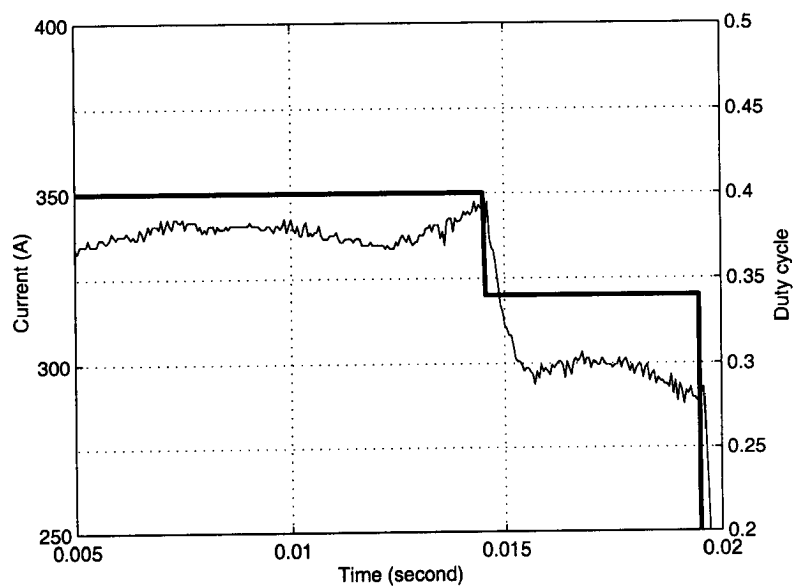


Figure 5.9: Plot of current and duty cycle step test

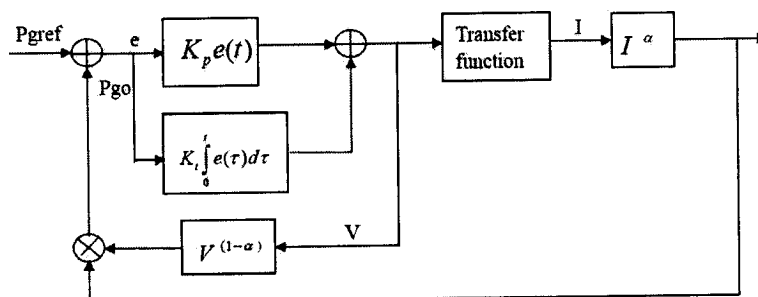


Figure 5.10: Block diagram for the PI controller tuning

5.4 Determining Set Point for each α

The goal of this experimental work is to show how using different weighted means of voltage and current as our controller variable effects the consistency of the welding process. In order to make this comparison valid, it is necessary that the welds have the same mean size. Thus it is necessary to find the mean size for our base operating condition, i.e open loop voltage control with a 45% duty cycle. In addition it is necessary to determine the set points for the other weighted means that achieve identical mean weld sizes.

To achieve this, first 40 welds were undertaken with the duty cycle of the welder fixed at 45% and 24ms welding time. The nugget size of 20 of the welds, and the tensile strength of 20 of the welds were then measured. The means were then calculated. In addition, the currents were measured during these welds and a mean current was determined to be 265A. Initial estimates of the set point were then evaluated as

$$\hat{P}_g(\alpha) = 6.1^{1-\alpha} \times 265^\alpha \quad (5.9)$$

Under the pure current control ($P_g = 265$), twelve welds were done at {94%, 96%, 98%, 100%, 102%, 104%, 106%} of these values. The mean nugget size at each of the set points were calculated. Table 5.1 lists the mean nugget diameters under different current settings. The two points closest to the mean achieved with open loop control were determined, and the actual operating set point (260.8amps) was determined by linearly extrapolating between those points. (see analysis section in the next chapter).

Switched to the generic power control mode (Figure 3.1), the set points P_g were evaluated as

$$P_g(\alpha) = 6.1^{1-\alpha} \times 260.8^\alpha \quad (5.10)$$

Table 5.1: Mean nugget size at different current set points

Current unit (amps)	Nugget size (mm)
250	0.2868
255	0.2912
260	0.3012
265	0.3220
270	0.3329
275	0.3147
280	0.3810

where α was changed from 0.1 to 0.9. Table 5.2 lists the corresponding set points at each of the α value.

Table 5.2: Set points at different α value

α	Set points P_g	α	Set points P_g
0.1	8.88	0.6	58.07
0.2	12.93	0.7	84.53
0.3	18.82	0.8	123.06
0.4	27.40	0.9	179.15
0.5	39.89	1.0	260.8

5.5 Variance Calculations

Finally, 80 welds were done at each of the identified set points with the appropriate weld power controller. Forty of the resulting welds were used to measure weld nugget size and 40 had tensile strength tests performed. The means and variances were then calculated for the experimental analysis which will be investigated in the next

chapter. Besides, the variance in each of the control variables with the corresponding weld power controllers was also collected for the controller analysis.

Chapter 6

Experimental Analysis and Results

6.1 Lobe Test for Open Loop Voltage Control Mode

Under the open loop voltage control mode, the weld strength and nugget size were measured for different voltage levels (PWM duty cycle), weld force and weld time. Figure 6.1 shows the plots of weld strength or nugget diameter versus weld time with force fixed at 1.5lb. As shown in this figure, increasing weld time increased the weld strength, and then decreased the joint strength, which may be the result of expulsion. At 40% duty cycle, expulsion appeared at a weld time of about 27 – 29ms, and the largest nugget size was obtained at 26ms. While at 45% duty cycle, expulsion was experienced earlier when the weld time was at approximately 24 – 26ms corresponding to the weld of maximum nugget diameter produced at 23ms. For 50% duty cycle, expulsion started before about 23ms.

The best weld time setting should be the one achieving the largest nugget size with little chance for expulsion. And expulsion was estimated in real time through the dynamic resistance profile produced by the tip voltage and weld current signal from sensing circuits. The main indicator for expulsion is the instantaneous drop in the resistance (Figure 6.2).

A lobe curve that characterizes a weldability during resistance spot welding was then built. This is a three dimensional curve. One slice of this curve is given in Figure 6.3 the plot of duty cycle (voltage setting) and weld time for the force of $1.5lb$ is presented. Welds made with duty cycle and time below the lower curve have insufficient nugget size and therefore are considered unacceptable. Welds made with duty cycle and time exceeding the upper curve experience expulsion on welding and are likewise considered unacceptable. Only welds made with duty cycle and time lying within the lobe area are acceptable. Based on the lobe diagram, the best operating point for open loop voltage control mode (45% duty cycle, 24ms weld time and 1.5lb weld force) was achieved.

40 welds were undertaken with the operating condition of the best point, the mean nugget size $0.3055mm$ corresponding to a $80.75N$ weld strength of the welds was measured. In addition, the currents were measured during these welds and a mean current was determined to be $265A$. So the initial estimates of the set points were evaluated as Equation 5.9.

6.2 Step Test for Constant Current Control

Mode

Under the pure current control, the set point (P_g) was only specified as the current setting ($I = 265$). A PI controller was tuned manually based on the simulink model given in Figure 5.10 with the pure current control ($\alpha = 1$). The PI controller that gave 7.9% overshoot with fastest rise time was achieved (Figure 6.4). The corresponding gain K_p was 265, and K_I was 65000.

Twelve welds at {250, 255, 260, 265, 270, 275, 280} amps of the current settings

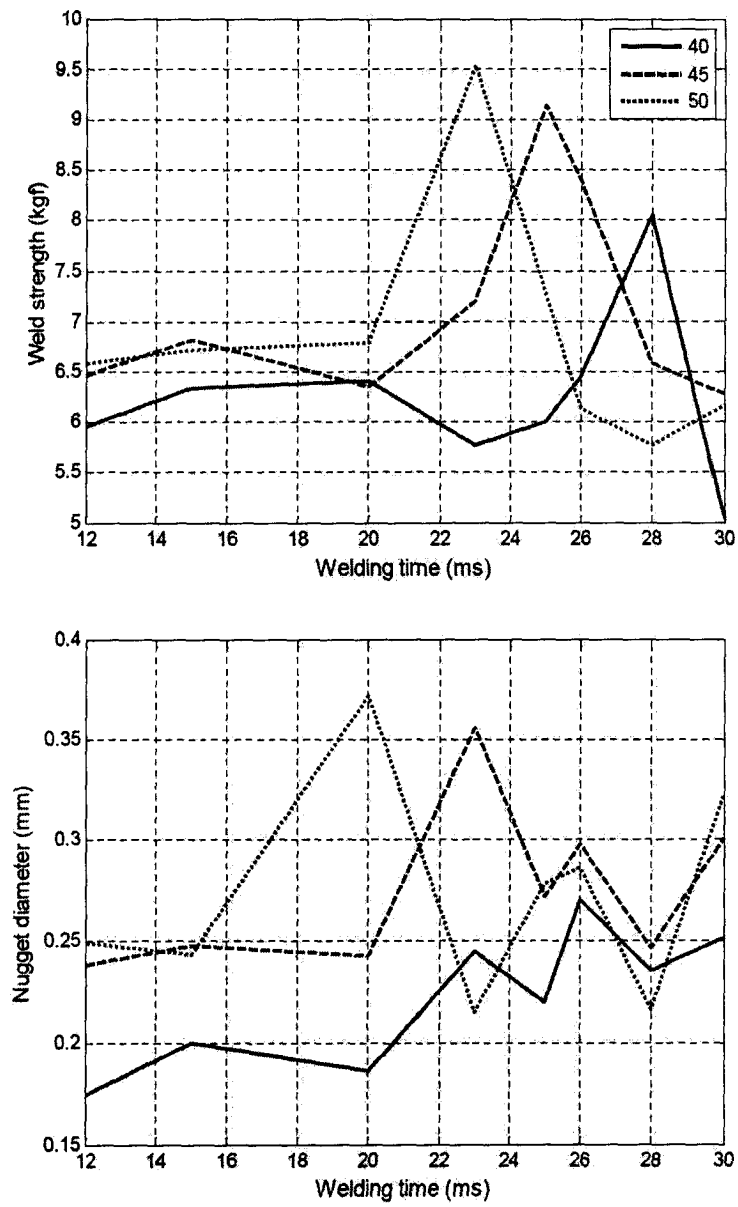


Figure 6.1: (a) Weld strength and (b) nugget diameter versus welding time

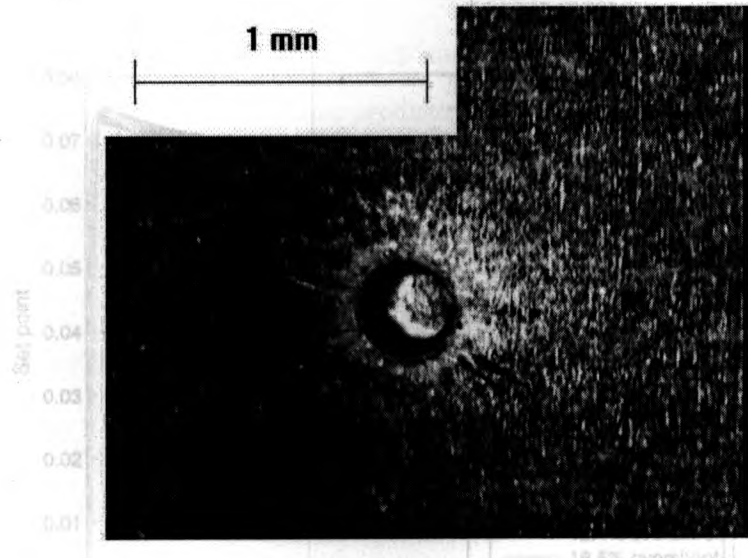
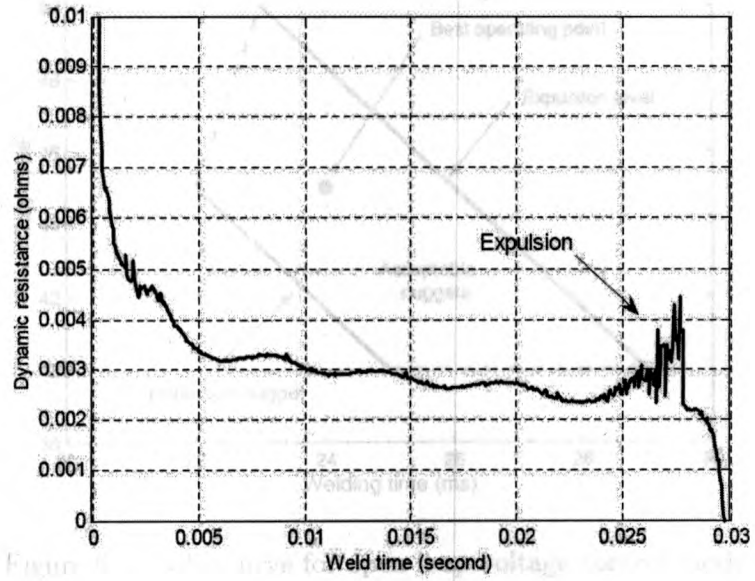


Figure 6.2: Effect of expulsion on dynamic resistance curve

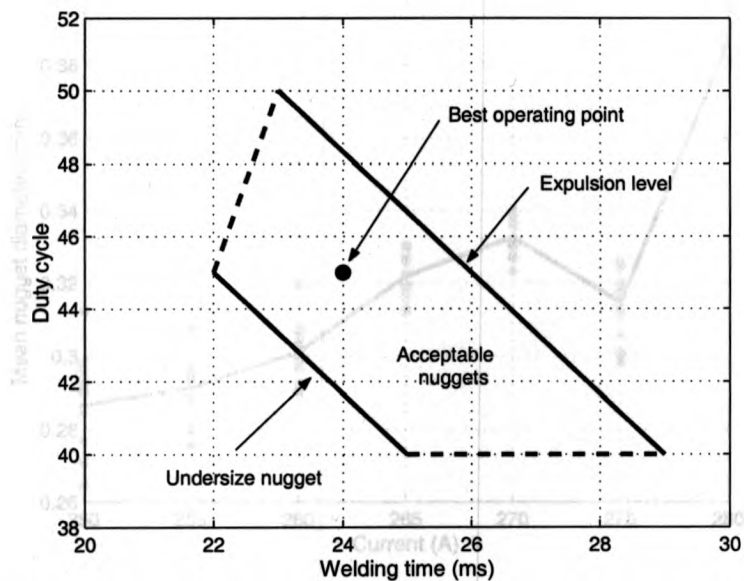


Figure 6.3: Lobe curve for open loop voltage control mode

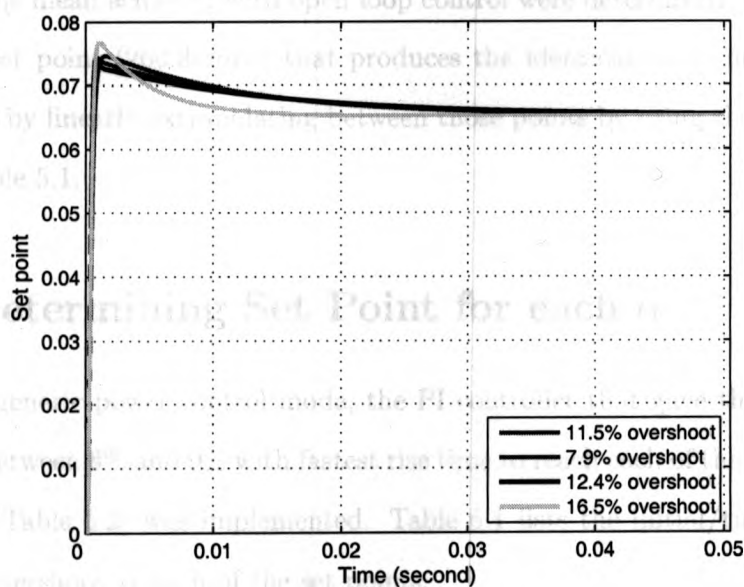


Figure 6.4: PI controller tuning for current control mode

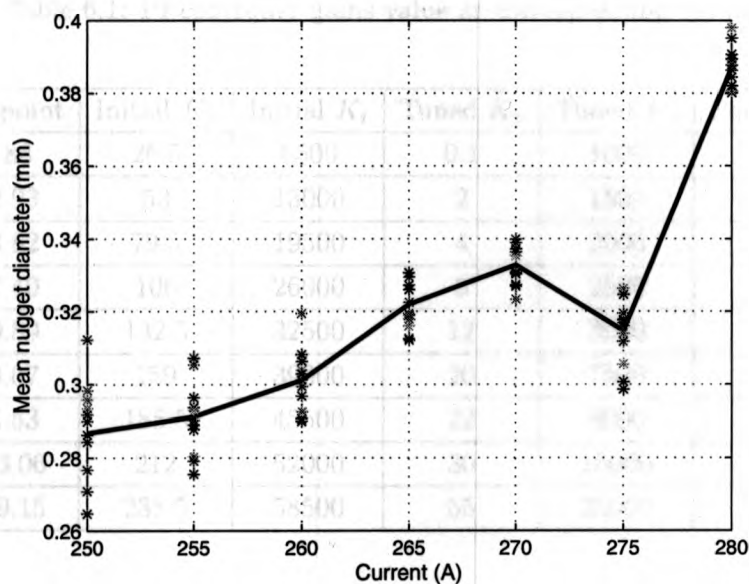


Figure 6.5: Mean nugget diameter for different current setting

were done. The mean nugget size were then calculated (Figure 6.5). The two points closest to the mean achieved with open loop control were determined, and the actual operating set point (260.8amps) that produces the identical mean nugget size was determined by linearly extrapolating between those points by using the experimental data in Table 5.1.

6.3 Determining Set Point for each α

Under the generic power control mode, the PI controller that gave the overshoot in the range between 6% and 9% with fastest rise time to reach each of the corresponding set points (Table 5.2) was implemented. Table 6.1 lists the initial/tuned controller gains and overshoot at each of the set points.

After doing eighty welds at each of the set point, Forty of the resulting welds

Table 6.1: PI controller gains value at corresponding set points

α	Set point	Initial K_p	Initial K_i	Tuned K_p	Tuned K_i	Percent overshoot
0.1	8.88	26.5	6500	0.1	1000	8.6%
0.2	12.93	53	13000	2	1500	6.2%
0.3	18.82	79.5	19500	4	2000	6.1%
0.4	27.40	106	26000	6	2500	6.6%
0.5	39.89	132.5	32500	12	3000	6.3%
0.6	58.07	159	39000	20	7500	8.9%
0.7	84.53	185.5	45500	22	8000	8.2%
0.8	123.06	212	52000	30	10000	8.3%
0.9	179.15	238.5	58500	55	25000	8.9%

were used to measure weld nugget size and 40 had tensile strength tests performed. The nugget size and weld strength were collected for the experimental analysis. Table 6.2 gives the value of the mean nugget diameter at each of the set points.

6.4 Experimental Data Analysis

Based on the experimental data from the welding tests, further statistic analysis has be performed. Two different variance has been studied: nugget size and weld strength. The variance in the nugget size is used to evaluate the general effect of the control variable on the welding quality. The smaller the variance, the less dispersion of the samples, and more consistent the weld quality. While the variance in the weld strength is another available indicator of the weld quality. The variance of nugget size or weld strength is expressed as:

$$\sigma_a^2 = \frac{1}{n} \sum_{i=1}^n (A_i - \hat{A})^2 \quad (6.1)$$

Table 6.2: Mean nugget diameter at different set points

α	Set point	Mean nugget size(mm)
0	6.1	0.3055
0.1	8.88	0.3092
0.2	12.93	0.3085
0.3	18.82	0.3079
0.4	27.40	0.3064
0.5	39.89	0.3044
0.6	58.07	0.3049
0.7	84.53	0.3079
0.8	123.06	0.3074
0.9	179.15	0.3102
1	260.8	0.3055

where, A_i is the diameter or weld strength of the nugget sample i , \hat{A} is the mean of the nugget diameters or weld strength, and σ_a^2 is the variance.

The variance of nugget size and weld strength has been calculated initially and the results are illustrated in (Figure 6.6). When α is set to zero, 80 welds were done with 45% duty cycle for the entire weld time. The variance was calculated and shown in Figure 6.6. Then another 80 welds were done with 100% voltage set point for the first 0.4ms weld time as with the other experiments. Compared with the prior variance value, significant improvement was achieved when using the slower current rise time. Moreover, it is obvious that increasing α initially decreases the variance of both nugget size and weld strength, and then increases the variance. When $\alpha = 0.6$, the variance in both nugget size and weld strength is the smallest. And with this control index, approximate 60% improvement in variance in weld nugget diameter versus constant current control ($\alpha = 1$) is achieved. The analysis results indicate that 60% weighting on the current or 40% weighting on the voltage produces the

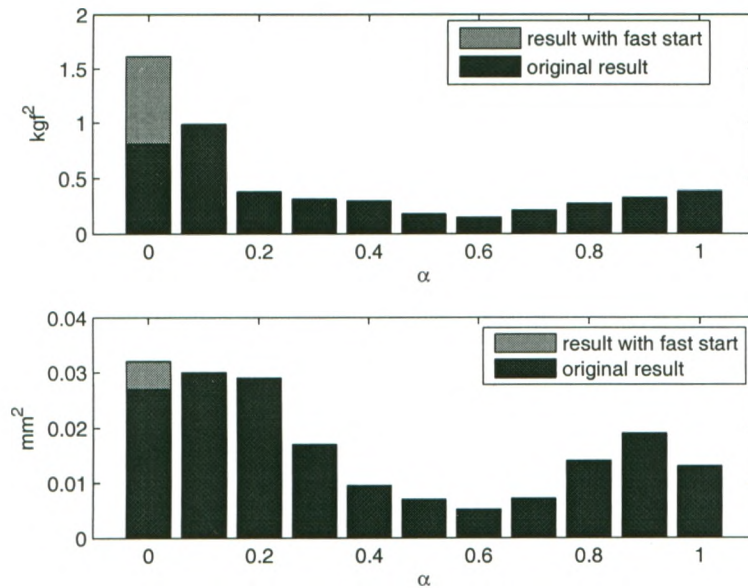


Figure 6.6: Variance comparison in (a) weld strength and (b) nugget diameter

most consistent weld nugget diameter and weld strength for this study.

The control variables for the appropriate power control modes are listed in Table 6.3. In order to compare the control modes, the variance of the control variable was calculated. The variance of the controlled variable is defined as:

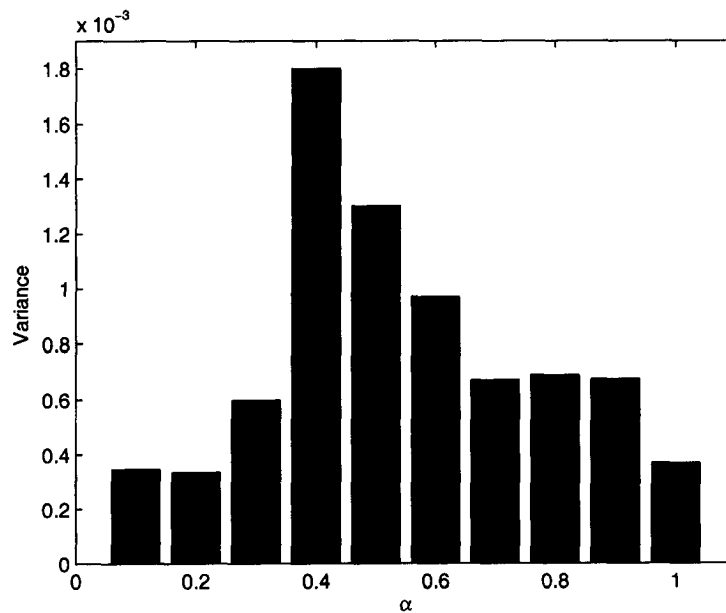
$$\sigma_c^2 = \frac{\frac{1}{n} \sum_{i=1}^n (V_i^{(1-\alpha)} I_i^\alpha - P(\alpha))^2}{P(\alpha)^2} \quad (6.2)$$

where, $V_i^{(1-\alpha)} I_i^\alpha$ is the average of the control variable of the nugget sample i at different α , $P(\alpha)$ is the desired power set point, and σ_c^2 is the variance.

For the open loop voltage control mode, the output voltage (duty cycle) was controlled directly. And the variance in control variable was then calculated as zero. Figure 6.7 shows the variances of control variables over the whole welding process under the each of the closed loop power control modes. It is indicated that the variance

Table 6.3: Control variables under the control modes

Control mode	Control variable
Open loop voltage control	Output voltage (Duty cycle)
Constant current control	Output current
Generic power control	Output power

Figure 6.7: Variance comparison in control variables at each of α

is the smallest when α is set to 0.2, while when α is equal to 0.4, the variance is the highest. The analysis shows that the improvement of welding consistency seen at with the optimal control strategy was not a result of better controller implementation at that point.

6.5 Summary of The Experiments

- Lobe tests for open loop voltage control mode have been performed firstly to determine adequate variables and best operating point ensuring the welding quality.

- Duty cycle of the PWM: 45%

- Welding time: 24ms

- Weld force: 1.5lb

- After doing forty welds at this set point, the mean nugget size was achieved. Meanwhile the output currents were obtained from the sensing circuit. Then the mean current was determined as 265A. So the initial estimates of the set points were then evaluated as:

$$\hat{P}_g(\alpha) = 6.1^{1-\alpha} \times 265^\alpha.$$

- Under the pure current control mode ($P_g = 265$), a PI controller was tuned manually to get 7.9% overshoot with fastest rise time.
- At {94%, 96%, 98%, 100%, 102%, 104%, 106%} of these values, twelve welds were then done. By using the experimental data from the welding test, the actual set point (260.8) that produced identical mean nugget diameter with the best operating point was achieved.
- The set points for the remain α were then evaluated as:

$$P_g(\alpha) = 6.1^{1-\alpha} \times 260.8^\alpha.$$

- At each of the set points, the PI controller was tuned to get 6% – 9% overshoot with maximizing the speed of response. A series of experiments were conducted

around these operating points to experimentally determine the set point that produced the same nugget size as used for constant current and constant voltage controllers. Then 80 welds were done at each of the identified set points. Forty of the resulting welds were used to measure weld nugget size and 40 had tensile strength tests performed. The means and variances were then calculated.

- Two variances for evaluating weld quality have been studied:
 - Variance of nugget diameter representing the welding quality;
 - Variance of weld strength confirming the results of weld strength.
- Analysis of the variance of nugget size indicated that among the different control variable for the generic power control mode under study, the best welding quality was achieved when $\alpha = 0.6$.
- Analysis of the variance of weld strength demonstrated similar improvement in weld quality and confirmed the results with the variance in nugget diameter analysis.
- For comparing the closed-loop power controllers, analysis of the variance of control variable concluded that the proceeding result was not a result of the quality of the controller design.

Chapter 7

Conclusion and Future Work

7.1 Summary of Achievements

Based on the detailed discussion on experimental design and data analysis results, the main achievements of this thesis are:

- A new power supply strategy to improve the consistency of resistance spot welding for every spot weld was investigated. And a generic power control mode has been discussed and implemented for the resistance spot welding process. The implemented three control modes, voltage control, current control and power control modes can be seen as three special points in this generic power control mode.
- The power supply for small scale RSW in this study was described. A hall effect current sensor was built. So the load current analog signal was measured to support implementing the control schemes. The power supply is a pulse width modulated DC-DC converter. Thus its nominal output is given by the duty cycle times the maximum voltage of $13.5V$.
- An experimental approach for finding the optimum control variable for resistance spot welding was investigated. For $0.152mm$ thick stainless steel coupons, the weld quality under different control variables has been analyzed based on

the experimental data. The results demonstrated that a 40% weighting on the voltage produced the most consistent welds. With this control variable, substantial improvement in variance in nugget size compared with constant current control was achieved.

- The stability of the different closed loop power control modes has been analyzed based on the experimental data. The results indicated that the control scheme with $\alpha = 0.2$ is the most stable one among the control modes under study.

Note the obvious benefit of this approach is more consistent welds, but it can also be used to achieve stronger welds. By making the welding process more consistent, the weld lobe should be enlarged. That is the range in which expulsion occasionally occurs should become smaller, shifting the upper band of the lobe curve to higher current and time. Thus, the base operating condition can be made more aggressive, without increasing the number of welds compromised by expulsion.

7.2 Future Work

Based on the achievements of this thesis, the following tasks are recommended for further research and study:

- In Figure 6.6, significant variance improvement was achieved when using slower current rise time. So an initially varying power set point or PI controller with anti-windup features should be used.
- The new power supply control strategy can be applied for other specific weld geometry. And the potential for this approach for different weld materials can be compared .

- This strategy can be pursued for commercial welding system to broaden the upper band of the lobe curve to higher current and time to achieve more powerful base operating condition.
- Further improvement in the welding process can be made by replacing the nominal voltage as given by the duty cycle times the open circuit voltage by actually tip voltage measurements. The generic power control mode can be improved to control the tip voltage with little modifications.
- Instead of controlling the output voltage, the tip voltage can be controlled based on the improved control mode. And for one specific weld geometry, the same experimental approach can be followed to pursue the optimum control variable. This should have the effect of substantially reducing the variance for constant voltage control and changing the curves seen in Figure 6.3 to move the minimum to left.

Bibliography

- [1] X. T. Zhang, "Operating condition identification and electrode condition monitoring in resistance spot welding process," Master's thesis, The University of Western Ontario, London, ON, Canada, 2002.
- [2] B. H. Chang, M. V. Li, and Y. Zhou, "A comparative study of 'small-scale' and 'large scale' resistance spot-welding ," *Science and Technology of Welding and Joining*, vol. 6, pp. 273–280, 2001.
- [3] A. G. Livshits, "Universal quality assurance method for resistance spot welding based on dynamic resistance ," *Welding Journal*, vol. 76, pp. 383–390, 1997.
- [4] R. T. Wood, L. W. Bedard, J. F. Bedard, B. M. Bernstein, J. Czechowski, M. M. D'ndrea, and R. A. Hogle, "A closed-loop control system for three-phase resistance spot welding," *Welding Journal*, vol. 64, pp. 26–30, 1985.
- [5] N. T. Williams, "Use of voltage integration for monitoring and feedback," *Resistance Welding Control and Monitoring*, vol. 2, pp. 13–18, 1997.
- [6] J. Heb, T. Kem, W. Krigl, and M. Schweizer, "Visualization of the resistance spot welding process in the production line," *Welding Journal*, vol. 77, pp. 495–502, 1998.
- [7] S. R. Patange, T. Anjaneyulu, and G. P. Reddy, "Microprocessor-based resistance spot welding monitor," *Welding Journal*, vol. 64, pp. 33–38, 1985.
- [8] D. W. Steimier, "Downsizing in the world of resistance spot welding ," *Welding Journal*, vol. 77, pp. 39–47, 1998.
- [9] L. J. Brown and J. Lin, "Power supply designed for small-scale resistance spot welding," *Welding Journal*, vol. 84, pp. 25–28, 2005.
- [10] G. R. Archer, "A new system for automatic feedback control of resistance spot welding," *The International Journal of Advanced Manufacturing Technology*, vol. 38, pp. 987–993, 1999.
- [11] W. L. Roberts, "Resistance variations during spot welding," *Welding Journal*, vol. 30, pp. 1004–1019, 1951.
- [12] J. S. Moon, G. S. Kim, J. M. Kim, and C. Y. Won, "Power control of resistance spot welding system with high dynamic performance," *Industrial Electronics, Control and Instrumentation*, vol. 2, pp. 845–849, 1997.

- [13] J. Lin, "Power supply designed for small-scale resistance spot welding," Master's thesis, The University of Western Ontario, London, ON, Canada, 2005.
- [14] N. T. Willian, *ASM HANDBOOK: Welding, brazing and soldering*. ASM International, 1993, vol. 6.
- [15] W. Li, S. J. H, and J. Ni, "On-line quality estimation in resistance spot welding," *Journal of Manufacturing Science and Engineering*, vol. 122, pp. 511-512, 2000.
- [16] Y. Zhou, S. J. Dong, and K. J. Ely, "Weldiability of thin sheets metals by small-scale resistance spot welding using high-frequency inverter and capacitor-discharge power supply," *Journal of Electrical Materials*, vol. 30, 2001.
- [17] D. W. Dickinson, J. E. Franklin, and A. Stanya, "Characterization of spot welding behavior by dynamic electrical parameter monitoring," *Welding Journal*, vol. 59, pp. 170-176, 1980.
- [18] K. Ely and Y. Zhou, "Microresistance spot welding of Kovar, steel, and nickel," *Science and Technology of Welding and Joining*, vol. 6, pp. 63-72, 2001.
- [19] J. E. Gould, "Welding research supplement," *Welding Journal*, vol. 66, pp. 1-10, 1987.
- [20] J. G. Kaiser, G. L. Dunn, and T. W. Eagar, "Welding research supplement," *Journal of Electrical Materials*, vol. 61, pp. 167-174, 1982.
- [21] D. W. Dickson, J. E. Franklin, and A. Stanya, "Welding research supplement," *Journal of Electrical Materials*, vol. 59, pp. 170-196, 1980.
- [22] Y. Zhou, P. Gorman, W. Tan, and K. J. Ely, "Weldiability of thin sheet metals during small-scale resistance spot welding using an alternating-current power supply," *Journal of Electrical Materials*, vol. 29, pp. 1090-1099, 2000.
- [23] A. V. Demnsion, D. J. Toncich, and S. Masood, "Control and process-based optimisation of spot-welding in manufacturing systems," *The International Journal of Advanced Manufacturing Technology*, vol. 13, pp. 256-263, 1997.
- [24] H. Zhang and J. Senkara, *RESISTANCE WELDING: Fundamentals and Applications*. CRC Press, Taylor & Francis Group, 2006.
- [25] N. Malbotra, "Online tip voltage and resistance measurement in RSW process," Master's thesis, The University of Western Ontario, London, ON, Canada, 2005.
- [26] L. J. Brown and Y. J. Sun, "Tuning to Stabilize Adaptive Internal Model Controller for Periodic Disturbance Cancellation," *IEEE Conference on Decision and Control*, vol. 9, pp. 1914-1919, 2006.

- [27] L. J. Brown and J. S. Schwaber, "Identifying operations from pre-weld information for resistance spot welding," *Proceedings of the American Conference*, 2000.
- [28] D. F. Farson, J. Z. Chen, K. Ely, and T. Frech, "Monitoring resistance spot nugget size by electrode displacement," *Journal of Manufacturing Science and Engineering*, vol. 126, pp. 3911–394, 2004.
- [29] J. Bai, L. J. Brown, M. Salem, and M. Kuntz, "Improved consistency of resistance spot welding via power supply control strategy," *Materials Science & Technology 2008 Conference and Exhibition, Pittsburgh, Pennsylvania*, 2008.
- [30] E. W. Kim and T. W. Eagar, "Parametric analysis of resistance spot welding lobe curve," *International Congress and Exposition*, vol. 97, pp. 107–118, 1989.
- [31] N. S. Nise, *Control Systems Engineering*, 4th ed. John Wiley & Sons. Inc, 2004.
- [32] F. G. B. C. Kuo, *Automatic Control System*. Copyright John Wiley and Sons Inc, 2003.
- [33] H. S. Chang, Y. J. Cho, S. G. Choi, and H. S. Cho, "A proportional-integral controller for resistance spot welding using nugget expansion," *Journal of Dynamic System, Measurement and Control*, vol. 111, pp. 333–336, 1989.

Appendix A
Experimental Results for Different
Control Schemes

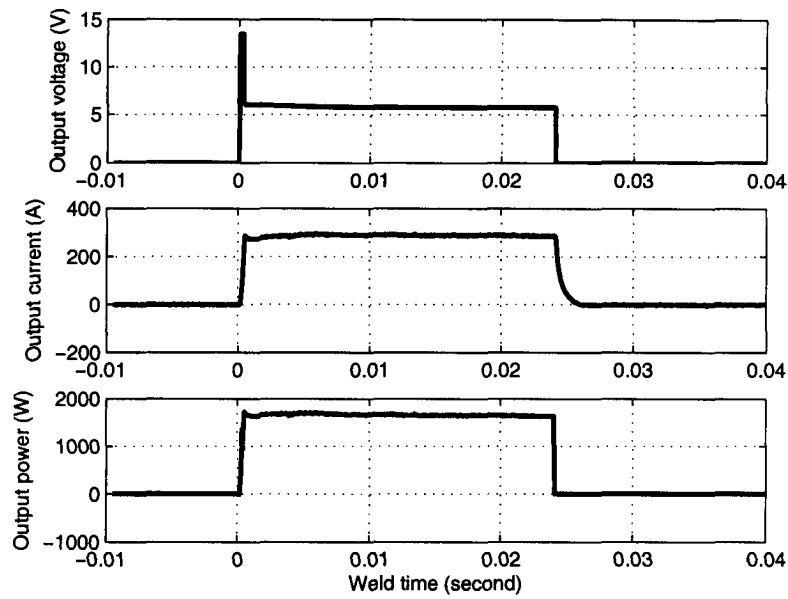


Figure A.1: Experimental results for the control mode with $\alpha = 0.1$

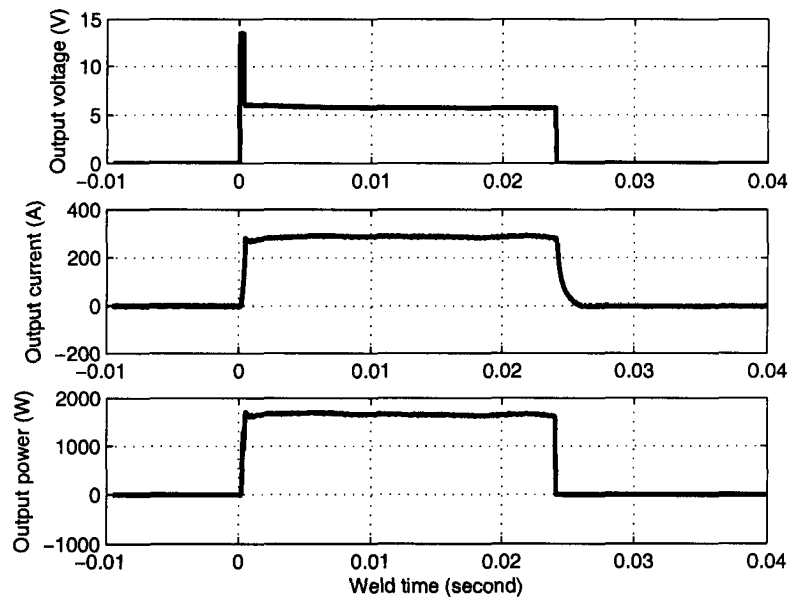


Figure A.2: Experimental results for the control mode with $\alpha = 0.2$

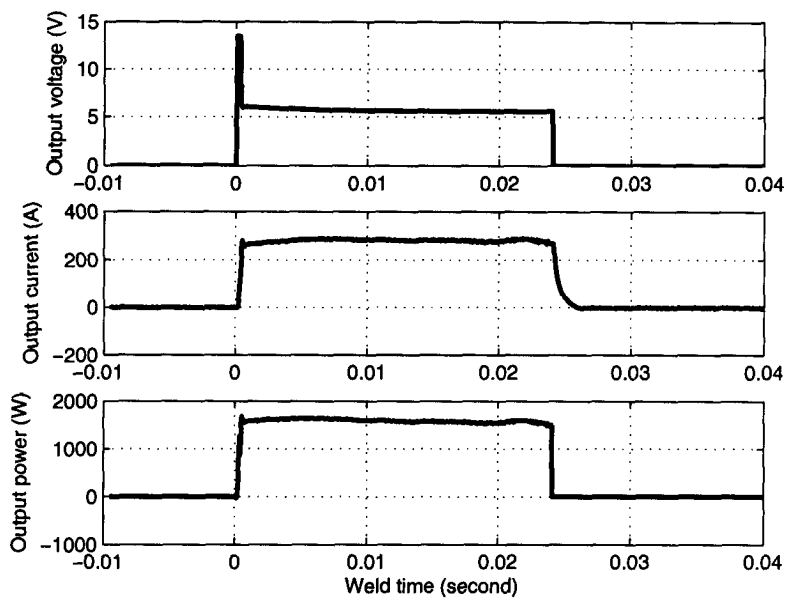


Figure A.3: Experimental results for the control mode with $\alpha = 0.3$

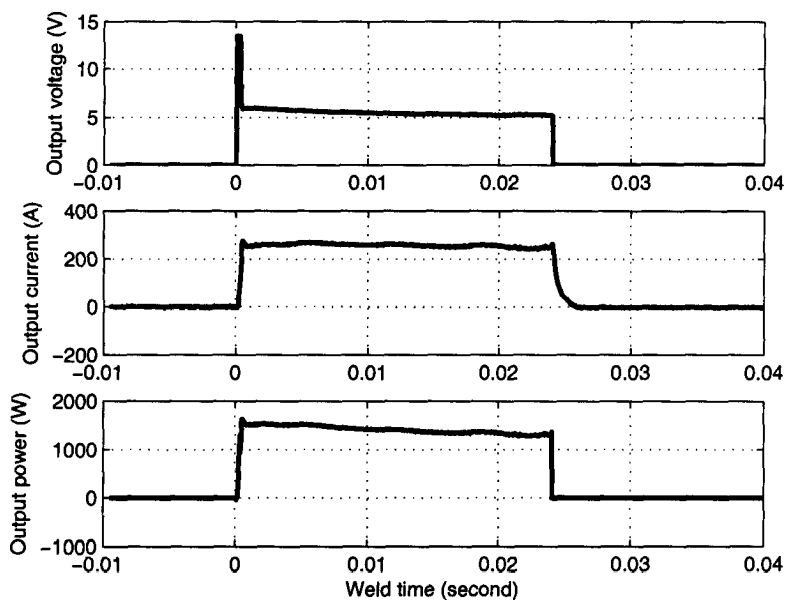


Figure A.4: Experimental results for the control mode with $\alpha = 0.4$

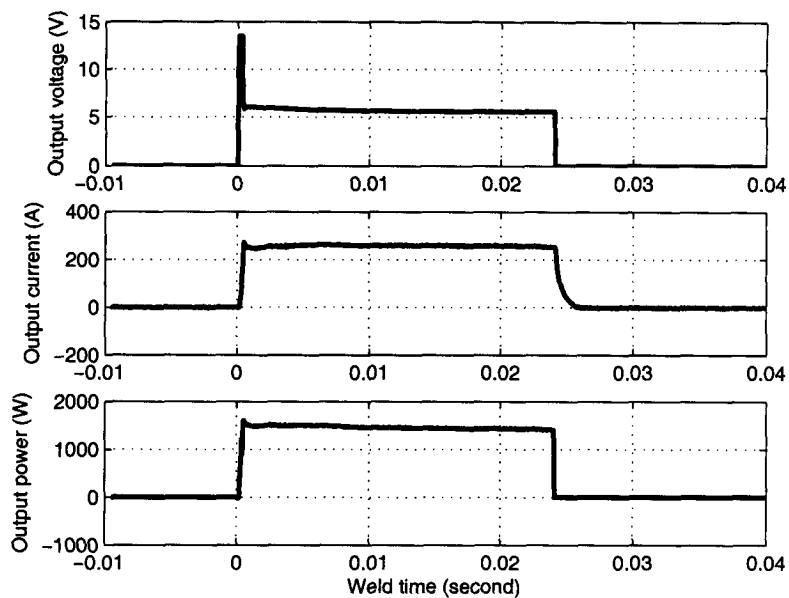


Figure A.5: Experimental results for the control mode with $\alpha = 0.6$

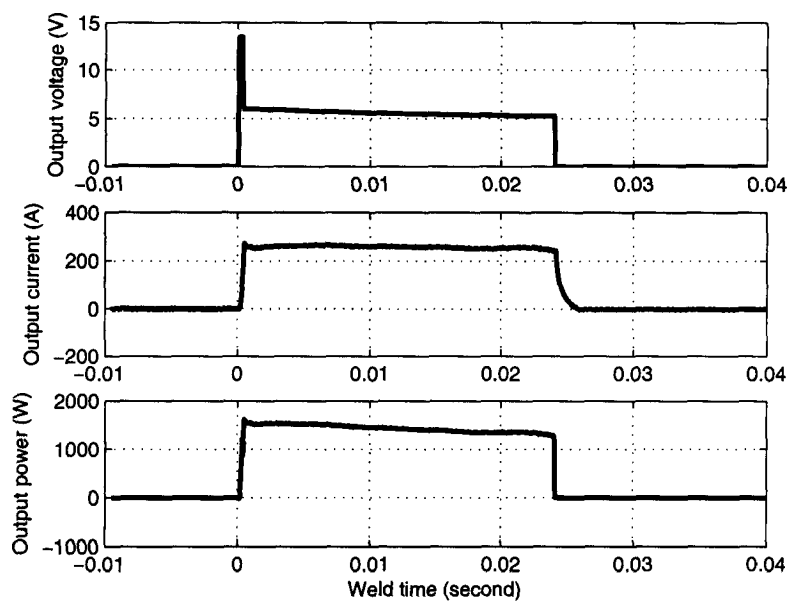
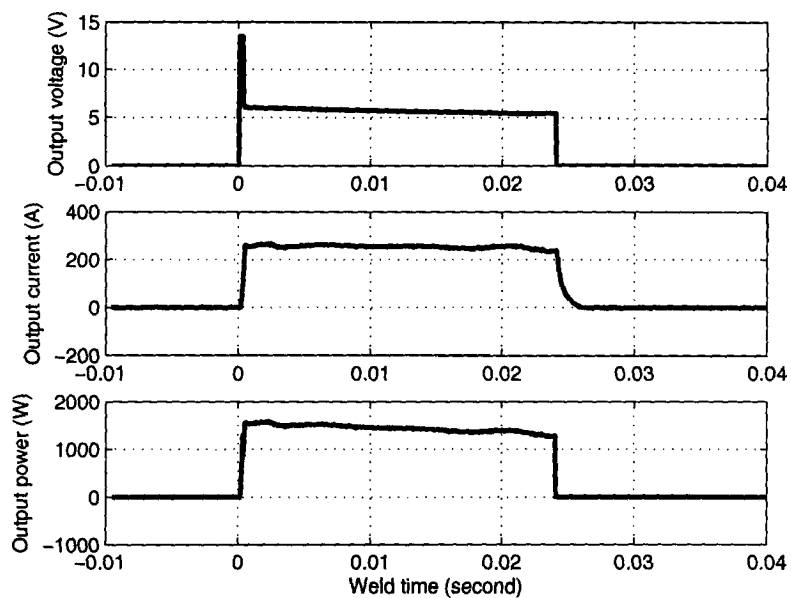
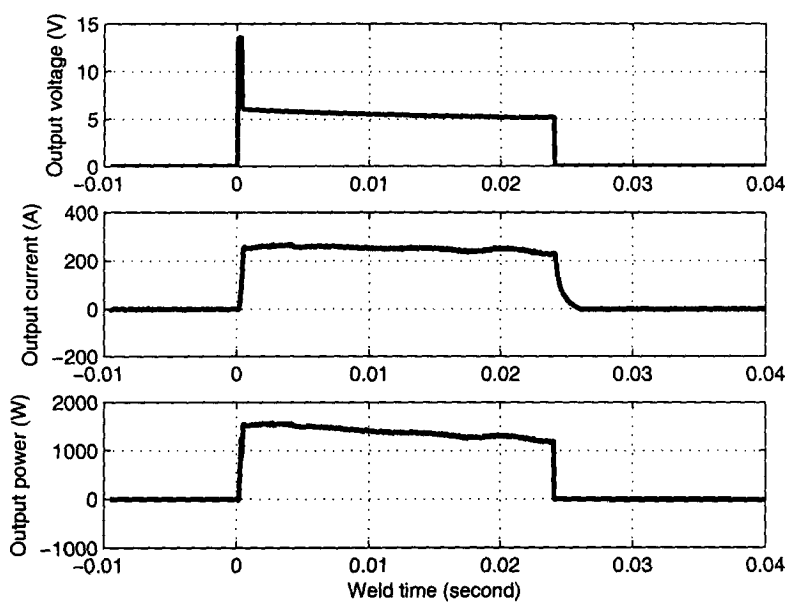


Figure A.6: Experimental results for the control mode with $\alpha = 0.7$

Figure A.7: Experimental results for the control mode with $\alpha = 0.8$ Figure A.8: Experimental results for the control mode with $\alpha = 0.9$